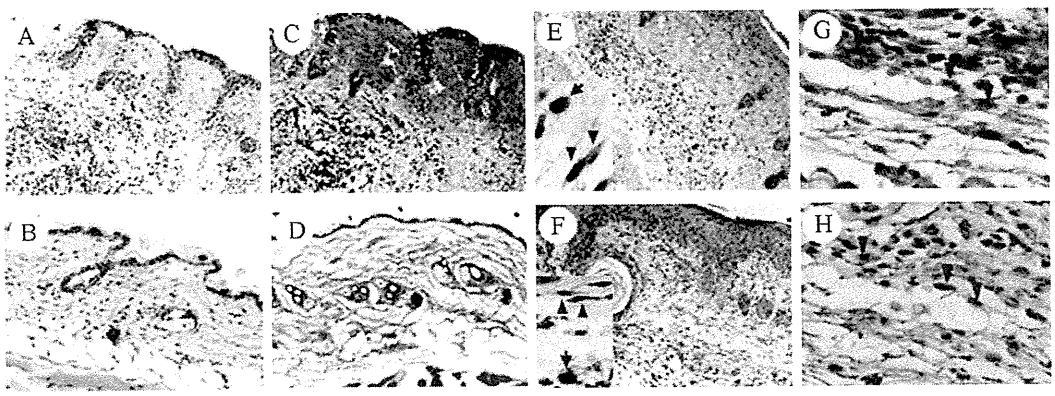

Fig. 1. Histopathological analysis of BMT skin tissues. (A, C, E–H) Skin tissue from Scl GVHD murine skin ($n=5$), (B, D) Skin tissue from TCD-BMT murine skin ($n=5$). (A, B) HE staining. (C, D) Masson Trichrome staining. (E, F) Immunostaining with anti-AIF-1 Ab and anti-IL-6 Ab, respectively. (G, H) Fibroblasts are stained by AIF-1 and collagen I, respectively. Fibroblasts stained by anti-collagen I Ab have morphologically branched or demonstrate a spindle shaped cytoplasm with an elliptical nucleus (arrowhead). Mononuclear cells are mostly round with round nuclei (arrow). The same fibroblasts were stained both in sequential paraffin slices. (A–D) magnification ×40. (E, F) magnification ×40 and ×400. (G, H) magnification ×400.

3. Results

3.1. Immunohistochemical analysis of Scl GVHD murine skin

Allogeneic BMT mice had significantly lower body weights than TCD-BMT mice from day 10 after BMT (data not shown). We demonstrated the extent of thickened skin in these mice histologically. On day 21 after BMT, at an early stage of GVHD with hair loss, Scl GVHD mice showed a mixture of large pale oval numerous mononuclear cells and spindle shaped fibroblasts that infiltrated thickened skin compared with TCD-BMT mice (Fig. 1A and B). Fibrosis of the thickened dermal layer was also stained blue by Masson Trichrome (Fig. 1C and D). Spindle shaped cells of the thickened dermal layer were stained by anti-collagen I Ab. These fibroblasts also expressed AIF-1 in serial sections (Fig. 1E, G and H). Moreover, we found significantly enhanced expression of AIF-1 in infiltrating mononuclear cells and fibroblasts (histopathological score; mean ± SE, 2.83 ± 0.17) in Scl GVHD murine skin tissues. In contrast, the level of AIF-1 expression in infiltrating mononuclear cells and fibroblasts was low (histopathological score; mean ± SE, 0.58 ± 0.10) in TCD-BMT murine skin tissues (Fig. 2A). We also found significant expression of IL-6 in these cells of Scl GVHD skin (histopathological score; mean ± SE, 2.58 ± 0.17) compared with TCD-BMT skin (histopathological score; mean ± SE, 0.58 ± 0.10) (Figs. 1F and 2B). Immunostaining of tissue sections with normal rabbit serum was completely negative in all skin tissues (data not shown).

As seen in Fig. 3, Western blot analysis detected AIF-1 protein at 17 kDa as a single band in protein extracts from skin tissues of Scl GVHD, TCD-BMT, and normal mice. The intensity of AIF-1 protein band was greatly enhanced in the skin of Scl GVHD mice compared with that in TCD-BMT (Fig. 3A) and normal mice (data not shown). The IL-6 detected at 28 kDa, was also more highly expressed in Scl GVHD mice than in TCD-BMT mice (Fig. 3B) and normal mice (data not shown).

3.2. IL-6 secretion from NHDF by rAIF-1 stimulation

The IL-6 and PDGF in the supernatant from cultured NHDF after rAIF-1 stimulation for 24 h were slightly elevated in spite of the dose of rAIF-1, but the increase in the IL-6 concentration induced by 100 ng/ml rAIF-1 stimulation was more significant than that by 1 ng/ml or 10 ng/ml rAIF-1stimulation (Fig. 4).

3.3. Migration and proliferation of dermal fibroblasts following rAIF-1 stimulation

We examined the effect of AIF-1 upon the cell migration and proliferation of normal human dermal fibroblasts (NHDF) by quantifying the wound closure area in a wound healing assay. Confluent monolayers of NHDF were scratched to form wound and cultured in the absence or presence of rAIF-1 or anti-AIF-1 Ab for 24 h. rAIF-1 resulted in the increased cell migration in a dose-dependent manner and induced a significant increase in these parameters as compared with the control (Fig. 5A and B). The effect of 100 ng/ml of rAIF-1 was similar to that of 100 ng/ml of LPS. In WST-1 assay, the cell proliferation of NHDF stimulated by rAIF-1 did not induce a significant increase compared with the positive control (Fibroblast Cell Medium) (data not shown). These findings indicate that rAIF-1 induce the migration of dermal fibroblast but not proliferation.

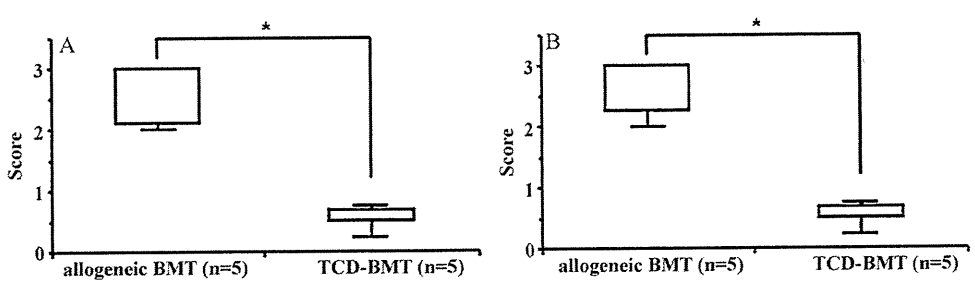

Fig. 2. Histopathological scores of immunoreactive AIF-1 and IL-6 in BMT skin tissues. A and B indicate the histopathological graded scores of the extent and intensity of immunostaining with anti-AIF-1 Ab and anti-IL-6 Ab, respectively, for allogeneic BMT skin tissues ($n=5$) and TCD-BMT skin tissues ($n=5$). The box plot includes an interquartile range (box), whereas the whiskers represent the 10–90th percentiles. The differences between two groups were analyzed by the Mann–Whitney U test. *$p<0.01$.

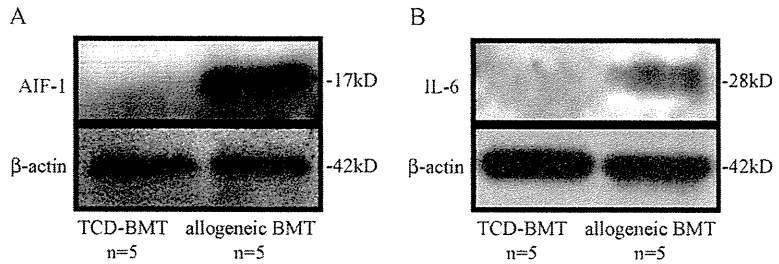

Fig. 3. Western blot analysis of AIF-1 and IL-6 in BMT skin tissues. Up-regulation of AIF-1 and IL-6 in skin tissues of Scl GVHD mice was detected compared with those of TCD-BMT mice by Western Blotting. (A) AIF expression, (B) IL-6 expression.

4. Discussion

In this study, we demonstrated that immunoreactive AIF-1 and IL-6 were significantly expressed in infiltrating mononuclear cells and fibroblasts in thickened skin of Scl GVHD mice compared with TCD-BMT mice. The immunohistochemical findings were confirmed by Western blot analysis. The effect of IL-6 production on NHDF by rAIF-1 was weak, despite which rAIF-1 increased the migration of NHDF directly. These findings suggest that AIF-1, which can induce the migration of fibroblasts and the production of IL-6 in affected skin tissues, is an important molecule promoting fibrosis in GVHD.

Allogeneic chronic GVHD presents with skin fibrosis like SSc [18]. Rapidly early cutaneous fibrosis which is one of the most critical pathological features in SSc is caused by the chemotactic migration of infiltrating mononuclear cells and fibroblasts [29]. In our study, AIF-1 was significantly expressed in infiltrating mononuclear cells and fibroblasts in thickened skin of Scl GVHD mice. AIF-1 was originally identified and cloned from rat cardiac allografts undergoing chronic rejection. To clarify the pathogenesis of GVHD it would be important to know how AIF-1 affects the migration and infiltration of those cells to target organs by chemotaxis. It has been recently shown that chemokine–chemokine receptor interactions such as CXCL12–CXCR4, CCL21–CCR7 induce the migration of fibrocytes or mesenchymal stem cells from bone marrow and play a role in the pathogenesis of tissue fibrosis [30,31]. There have been also many studies suggesting an association of bone marrow-derived cells with fibrosis [32,33]. These findings suggest that chronic fibroproliferative disorder is associated with various chemokines and chemokines affecting bone marrow-derived cells. So far, a relationship between AIF-1 and chemotaxis has been reported in some studies [14,34], but the AIF-1 was forcedly expressed by the stimulation of cytokines such as IFN-γ and TGF-β or by inserting the protein coding region of AIF-1 gene into cells [14,35]. We demonstrated that rAIF-1 itself has the function of chemotaxis in experiments with NHDF in a dose dependent manner. AIF-1 expressed in various tissues might be related to the pathogenesis of various immunoinflammatory diseases by the direct function of chemotaxis as we demonstrated.

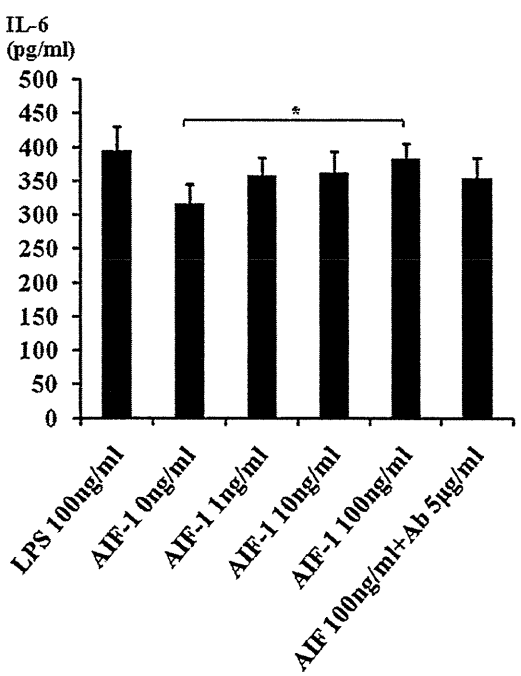

Fig. 4. IL-6 secretion from fibroblasts by rAIF-1. IL-6 concentration in the supernatant from cultured NHDF after rAIF-1 stimulation for 24 h. Each bar represents the mean ± SE of five experiments. The difference was analyzed by ANOVA followed by Bonferroni/Dunn's multiple comparison test. $^{*}p < 0.05$, $^{**}p < 0.01$.

IL-6 is a pleiotropic cytokine with multiple biological effects on immune regulation, haematopoiesis, inflammation, and oncogenesis, in addition to functioning as an autocrine or paracrine mediator on many cells [36]. We showed that rAIF-1 increased IL-6 production by synoviocytes, PBMCs [6]. In this study, IL-6 was also expressed in mononuclear cells and fibroblasts in the Scl GVHD model. Many reports have noted that PBMCs and fibroblasts of patients with SSc enhance induction of IL-6 [37] and that large amounts of serum IL-6 are strongly associated with the extent of skin and lung fibrosis in early SSc [38]. IL-6 induces increased production of collagen and glycosaminoglycans, hyaluronic acid and chondroitin-4/6-sulphates from human dermal fibroblasts [39]. Furthermore, IL-6 and TGF-β are inferred to lead to induction of IL-17 involved in the pathogenesis of SSc, because IL-17 induces inflammatory cytokines and cell adhesion molecules in fibroblasts, mononuclear cells, and endothelial cells [40,41]. AIF-1 may result in inducing cytokines and chemokines through secretion of IL-6, which leads to the migration of infiltrating inflammatory cells and fibroblasts.

We previously reported that rAIF-1 induces the proliferation of cultured synovial fibroblasts derived from RA in a dose-dependent manner [6]. It is also reported that AIF-1-transduced cells can enhance proliferation and can also promote entry into the cell cycle in the progression of the earliest phases (G1, G1/S transition) of the cell cycle, including cyclin E, cdks 6 and 7, and Skp1 [34]. In our inner preliminary study, skin dermal fibroblasts in primary culture from Scl GVHD mice did not show a significant migration and proliferation compared to those from control mice (data not shown). It is very difficult to demonstrate the function of dermal fibroblasts by use of primary culture in vitro because these cells were influenced by dealing with various reagents and conditions. However, the wound healing and WST-1 assays results that human rAIF-1 itself promoted the migration of dermal fibroblasts from human cell line but not the proliferation. These functions may be dependent on

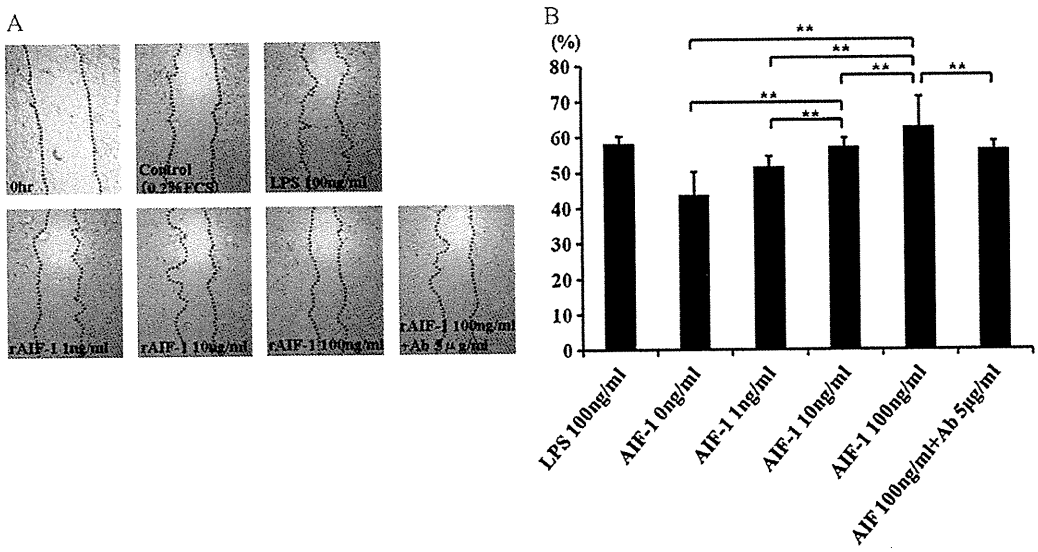

Fig. 5. AIF-1 increased NHDF migration. Scratch wounds of the confluent cell monolayer are cultured with or without AIF-1 or anti-AIF-1 Ab for 24 h. Each bar represents the mean ± SE of five experiments. Differences were analyzed by ANOVA followed by Bonferroni/Dunn's multiple comparison test. $^{**}p < 0.01$.

the types of cell and AIF. AIF protein we synthesized was named AIF-5 according to a new nomenclature of the AIF family of proteins [24]. This AIF splice variants IRT-1, G1, BART-1 are encoded in the same region of the BAT2 gene on chromosome 6 [5]. All variants contain a varying number of exons and transcripts. The modular architecture suggests that differential splicing mechanisms are responsible for the production of individual proteins. In addition, the migration was suppressed by adding anti-AIF-1 Ab as a neutralizing Ab. A receptor of AIF-1 has not been discovered yet and the mechanism of these actions will be further examined in the near future.

In conclusion, we suggest the possibility that AIF-1 may play an important role in the fibrosing process in Scl GVHD mice. The biological function of AIF-1 has not been completely elucidated, but it is sure that AIF-1 can induce IL-6 secretion on mononuclear cells and the chemotaxis of fibroblasts. AIF-1 may thus represent a new target for antifibrotic therapy in SSc as well as chronic GVHD. However, it is sure that not only fibroblasts but also macrophages, monocytes and lymphocytes produce IL-6 and various chemokines as factors inducing fibroblast activation and fibrosis. AIF-1 is thought to be one of these other responsible for fibroblast activation and fibrosis. The relationship between AIF-1 and these factors in the pathogenesis of GVHD needs to be pursued in the near future.

Acknowledgement

This study was supported by a Grant-in-Aid for Research (C) (No. 22591080) from The Ministry of Education, Culture, Sports, Science and Technology (MEXT) of Japan.

References

[1] Iris FJ, Bougueleret L, Prieur S, Caterina D, Primas G, Perrot V, et al. Dense Alu clustering and a potential new member of the NFB family within a 90 kilobase HLA class III segment. Nat Genet 1999;3:137–45.
[2] Autieri MV. cDNA cloning of human allograft inflammatory factor-1: tissues distribution, cytokine induction, and mRNA expression in injured rat carotid arteries. Biochem Biophys Res Commun 1996;228:329–76.
[3] Utans U, Arceci RJ, Yamashita Y, Russell ME. Cloning and characterization of allograft inflammatory factor-1: a novel macrophage factor identified in rat cardiac allografts with chronic rejection. J Clin Invest 1995;95:2954–62.
[4] Utans U, Quist WC, McManus BM, Wilson JE, Arceci RJ, Wallace AF, et al. Allograft inflammatory factor-1: a cytokine-responsive macrophage molecule expressed in transplanted human heart. Transplantation 1996;61:1387–92.
[5] Hara H, Ohta M, Ohta K, Nishimura M, Obayashi H, Adachi T. Isolation of two novel alternative splicing variants of allograft inflammatory factor-1. Biol Chem 1999;380:1333–6.
[6] Kimura M, Kawahito Y, Obayashi H, Ohta M, Hara H, Adachi T, et al. A critical role for allograft inflammatory factor-1 in the pathogenesis of rheumatoid arthritis. J Immunol 2007;178:3316–22.
[7] Del Galdo F, Maul GG, Jimenez SA, Artlett CM. Expression of allograft inflammatory factor 1 in tissues from patients with systemic sclerosis and in vitro differential expression of its isoforms in response to transforming growth factor-β. Arthritis Rheum 2006;54:2616–25.
[8] Otieno FG, Lopez AM, Jimenez SA, Gentiletti J, Artlett CM. Allograft inflammatory factor-1 and tumor necrosis factor single nucleotide polymorphisms in systemic sclerosis. Tissue Antigens 2007;69:583–91.
[9] Pawlik A, Kurzawski M, Szczepanik T, Dziedziejko V, Safranow K, Borowiec-Chłopek Z, et al. Association of allograft inflammatory factor-1 gene polymorphism with rheumatoid arthritis. Tissue Antigens 2008;72:171–5.
[10] Alkassab F, Gourh P, Tan FK, McNearney T, Fischbach M, Ahn C, et al. An allograft inflammatory factor 1 (AIF1) single nucleotide polymorphism (SNP) is associated with anticentromere antibody positive systemic sclerosis. Rheumatology (Oxford) 2007;46:1248–51.
[11] Takehara K. Pathogenesis of systemic sclerosis. J Rheumatol 2003;30:755–9.
[12] Duncan MR, Frazier KS, Abramson S, Williams S, Klapper H, Huang X, et al. Connective tissue growth factor mediates transforming growth factor beta-induced collagen synthesis: down-regulation by cAMP. FASEB J 1999;13:1774–86.
[13] Igarashi A, Nashiro K, Kikuchi K, Sato S, Ihn H, Grotendorst GR, et al. Significant correlation between connective tissue growth factor gene expression and skin sclerosis in tissue sections from patients with systemic sclerosis. J Invest Dermatol 1995;105:280–4.
[14] Kelemen SE, Autieri MV. Expression of allograft inflammatory factor-1 in T lymphocytes: a role in T-lymphocyte activation and proliferative arteriopathies. Am J Pathol 2005;167:619–26.
[15] Del Galdo F, Jiménez SA. T cells expressing allograft inflammatory factor 1 display increased chemotaxis and induce a profibrotic phenotype in normal fibroblasts in vitro. Arthritis Rheum 2007;56:3478–88.
[16] Orsmark C, Skoog T, Jeskanen L, Kere J, Saarialho-Kere U. Expression of allograft inflammatory factor-1 in inflammatory skin disorders. Acta Derm Venereol 2007;87:223–7.
[17] Tian Y, Jain S, Kelemen SE, Autieri MV. AIF-1 expression regulates endothelial cell activation, signal transduction, and vasculogenesis. Am J Physiol Cell Physiol 2009;296:256–66.
[18] Furst DE, Clements PJ, Graze P, Gale R, Roberts N. A syndrome resembling progressive systemic sclerosis after bone marrow transplantation. A model for scleroderma? Arthritis Rheum 1979;22:904–10.
[19] Zhang Y, McCormick LL, Desai SR, Wu C, Gilliam AC. Murine sclerodermatous graft-versus-host disease, a model for human scleroderma: cutaneous cytokines, chemokines, and immune cell activation. J Immunol 2002;168:3088–98.
[20] Rogai V, Lories RJ, Guiducci S, Luyten FP, Matucci-Cerinic M. Animal models in systemic sclerosis. Clin Exp Rheumatol 2002;26:941–6.
[21] McCormick LL, Zhang Y, Tootell E, Gilliam AC. Anti-TGF-beta treatment prevents skin and lung fibrosis in murine sclerodermatous graft-versus-host disease: a model for human scleroderma. J Immunol 1999;163:5693–9.
[22] Nagira T, Matthew SB, Yamakoshi Y, Tsuchiya T. Enhancement of gap junctional intercellular communication of normal human dermal fibroblasts cultured

on polystyrene dishes grafted with poly-N-isopropylacrylamide. Tissue Eng 2005;11:1392–7.
[23] Kawata E, Ashihara E, Kimura S, Takenaka K, Sato K, Tanaka R, et al. Administration of PLK-1 small interfering RNA with atelocollagen prevents the growth of liver metastases of lung cancer. Mol Cancer Ther 2008;7:2904–12.
[24] Deininger MH, Meyermann R, Schluesener HJ. The allograft inflammatory factor-1 family of proteins. FEBS Lett 2002;514:115–21.
[25] Yamada R, Sano H, Hla T, Hashiramoto A, Fukui W, Miyazaki S, et al. Auranofin inhibits interleukin-1β-induced transcript of cyclooxygenase-2 on cultured human synoviocytes. Eur J Pharmacol 1999;385:71–9.
[26] Furuya M, Kato H, Nishimura N, Ishiwata I, Ikeda H, Ito R, et al. Down-regulation of CD9 in human ovarian carcinoma cell might contribute to peritoneal dissemination: morphologic alteration and reduced expression of beta1 integrin subsets. Cancer Res 2006;5:2617–25.
[27] Kikuchi Y, Takai T, Ota M, Kato T, Takeda K, Mitsuishi K, et al. Application of immunoreaction enhancer solutions to an enzyme-linked immunosorbent assay for antigen-specific IgE in mice immunized with recombinant major mite allergens or ovalbumin. Int Arch Allergy Immunol 2006;141:322–30.
[28] Uchida H, Maruyama T, Ono M, Ohta K, Kajitani T, Masuda H, et al. Histone deacetylase inhibitors stimulate cell migration in human endometrial adenocarcinoma cells through up-regulation of glycodelin. Endocrinology 2007;148:896–902.
[29] Distler JH, Akhmetshina A, Schett G, Distler O. Monocyte chemoattractant proteins in the pathogenesis of systemic sclerosis. Rheumatology 2009;48:98–103.
[30] Mehrad B, Burdick MD, Strieter RM. Fibrocyte CXCR4 regulation as a therapeutic target in pulmonary fibrosis. Int J Biochem Cell Biol 2009;41:1708–18.
[31] Lama VN, Phan SH. The extrapulmonary origin of fibroblasts: stem/progenitor cells and beyond. Proc Am Thorac Soc 2006;3:373–6.
[32] Lin WR, Brittan M, Alison MR. The role of bone marrow-derived cells in fibrosis. Cells Tissues Organs 2008;188:178–88.
[33] Strieter RM, Gomperts BN, Keane MP. The role of CXC chemokines in pulmonary fibrosis. J Clin Invest 2007;117:549–56.
[34] Chen X, Kelemen SE, Autieri MV. AIF-1 expression modulates proliferation of human vascular smooth muscle cells by autocrine expression of G-CSF. Arterioscler Thromb Vasc Biol 2004;24:1217–22.
[35] Autieri MV, Carbone C. Expression of allograft inflammatory factor-1 is a marker of activated human vascular smooth muscle cells and arterial injury. Arterioscler Thromb Vasc Biol 2000;20:1737–44.
[36] Kishimoto T. The biology of interleukin-6. Blood 1989;74:1–10.
[37] Feghali CA, Bost KL, Boulware DW, Levy LS. Mechanisms of pathogenesis in scleroderma I. Overproduction of interleukin 6 by fibroblasts cultured from affected skin sites of patients with scleroderma. J Rheumatol 1992;19:1207–11.
[38] Hasegawa M, Sato S, Fujimoto M, Ihn H, Kikuchi K, Takehara K. Serum levels of interleukin 6 (IL-6), oncostatin M, soluble IL-6 receptor, and soluble gp130 in patients with systemic sclerosis. J Rheumatol 1998;25:308–13.
[39] Duncan MR, Berman B. Stimulation of collagen and glycosaminoglycan production in cultured human adult dermal fibroblasts by recombinant human interleukin 6. J Invest Dermatol 1991;97:686–92.
[40] Kurasawa K, Hirose K, Sano H, Endo H, Shinkai H, Nawata Y, et al. Increased interleukin-17 production in patients with systemic sclerosis. Arthritis Rheum 2000;43:2455–63.
[41] Murata M, Fujimoto M, Matsushita T, Hamaguchi Y, Hasegawa M, Takehara K, et al. Clinical association of serum interleukin-17 levels in systemic sclerosis: is systemic sclerosis a Th17 disease? J Dermatol Sci 2008;50:240–2.

Kawata et al. Journal of Clinical Bioinformatics 2011, 1:6
http://www.jclinbioinformatics.com/content/1/1/6

JCBi JOURNAL OF CLINICAL BIOINFORMATICS

REVIEW Open Access

RNA interference against polo-like kinase-1 in advanced non-small cell lung cancers

Eri Kawata[1,2], Eishi Ashihara[1,3*], Taira Maekawa[1]

Abstract

Worldwide, approximately one and a half million new cases of lung cancer are diagnosed each year, and about 85% of lung cancer are non-small cell lung cancer (NSCLC). As the molecular pathogenesis underlying NSCLC is understood, new molecular targeting agents can be developed. However, current therapies are not sufficient to cure or manage the patients with distant metastasis, and novel strategies are necessary to be developed to cure the patients with advanced NSCLC.

RNA interference (RNAi) is a phenomenon of sequence-specific gene silencing in mammalian cells and its discovery has lead to its wide application as a powerful tool in post-genomic research. Recently, short interfering RNA (siRNA), which induces RNAi, has been experimentally introduced as a cancer therapy and is expected to be developed as a nucleic acid-based medicine. Recently, several clinical trials of RNAi therapies against cancers are ongoing. In this article, we discuss the most recent findings concerning the administration of siRNA against polo-like kinase-1 (PLK-1) to liver metastatic NSCLC. PLK-1 regulates the mitotic process in mammalian cells. These promising results demonstrate that PLK-1 is a suitable target for advanced NSCLC therapy.

Introduction

Worldwide, approximately one and a half million new cases of lung cancer are diagnosed each year [1]. About 85% of lung cancer are non-small cell lung cancer (NSCLC), including adenocarcinoma, squamous cell, and large cell carcinoma [2], and NSCLC is the leading cause of cancer-related deaths. Surgery is generally regarded as the best strategy for lung cancers. However, only 30% of patients are suitable for receiving potentially curative resection [3], and it is necessary for other patients to be treated with chemotherapy. As we gain a better understanding of the molecular pathogenesis underlying NSCLC, new molecular targeting agents can be developed. Tyrosine kinase inhibitors (TKIs) targeting the epidermal growth factor receptor (EGFR), such as gefitinib and erlotinib, have shown remarkable activity in the patients with NSCLC, and particularly these TKIs are more effective to NSCLC with *EGFR* mutations in 19 exon (in-frame deletions) and exon 21 (L858R point mutation), which are found to be more prevalent in Asian patients [4,5]. However, despite the development of new TKIs, new mutations in *EGFR* exon 20, developing resistance to *EGFR* TKIs, have emerged in the treated NSCLC [6,7], and current therapies are not sufficient to cure or manage the patients with distant metastasis [8,9]. Therefore, novel strategies are necessary to be developed so that the patients with NSCLC can be cured.

RNA interference (RNAi) is a process of sequence specific post-transcriptional gene silencing induced by double-strand RNA (dsRNA) and this phenomenon was discovered in *Caenorhabditis elegans* (*C. elegans*) [10]. RNAi has been shown to function in higher organisms including mammals, and methods that exploit RNAi mechanisms have been developing. RNAi has now been well-established as a method for experimental analyses of gene function *in vitro* as well as in high-throughput screening, and recently, RNAi has been experimentally introduced into cancer therapy. To apply the RNAi phenomenon to therapeutics, it is important to select suitable targets for the inhibition of cancer progression and also to develop effective drug delivery systems (DDSs). Recently a lot of useful non-viral DDSs for small interfering RNAs (siRNAs) have been developed [11-17]. Besides selecting suitable targets, an important consideration for siRNA-mediated treatment is to predict and

* Correspondence: ash@koto.kpu-m.ac.jp
[1]Department of Transfusion Medicine and Cell Therapy, Kyoto University Hospital, Kyoto, Japan
Full list of author information is available at the end of the article

avoid off-target effects, which are the silencing of an unintended target gene, and potential immunostimulatory responses. To avoid those effects, the most specific and effective siRNA sequence must be validated. Modification of two nucleosides of the sense strand also completely co-inhibited the immunological activities of the antisense strand, while the silencing activity of the siRNA was maintained [18].

Polo-like kinase-1 (PLK-1) belongs to the family of serine/threonine kinases and regulates cell division in the mitotic phase [19,20]. PLK-1 is overexpressed in many types of malignancies and its overexpression is associated with poor prognosis of cancer patients [21,22]. In this review, we discuss possible RNAi strategies against PLK-1 in advanced lung cancers.

Mechanisms of RNAi

The precise mechanisms of RNAi are discussed in several reviews [23-25]. In the initiation phase of RNAi processes, following introduction of dsRNA into a target cell, dsRNA is processed into shorter lengths of 21-23 nucleotides (nts) dsRNAs, termed siRNAs, by the ribonuclease activity of a dsDNA-specific RNAse III family ribonuclase Dicer. Dicer consists of an N-terminal helicase domain, an RNA-binding Piwi/Argonaute/Zwille (PAZ) domain, two tandem RNAse III domains, and a dsRNA-binding domain [26,27]. Mammals and nematodes have only a single Dicer, which acts to produce both siRNAs and miRNAs [28-30], while other organisms have multiple Dicers which perform separate, specialized functions. *Drosophila* has two Dicers: *Drosophila* Dicer-1 is required for generating miRNAs, whereas *Drosophila* Dicer-2 produces siRNAs [25,31]. dsRNA precursors are sequentially processed by the two RNAse III domains of Dicer, and cleaved into smaller dsRNAs with 3' dinucleotide overhangs [26,32].

In the second effector phase, smaller dsRNAs enter into an RNA-induced silencing complex (RISC) assembly pathway [33]. RISC contains Argonaute (Ago) proteins, a family of proteins characterized by the presence of a PAZ domain and a PIWI domain [34]. The PAZ domain recognizes the 3' terminus of RNA, and the PIWI domain adopts an RNAse H-like structure that can catalyze the cleavage of the guide strand. Most species have multiple Ago proteins, but only Ago2 can cleave its RNA target in humans. The dsRNA is unwound by ATP-dependent RNA helicase activity to form two single-strands of RNA. The strand that directs silencing is called the guide strand, and the other is called the passenger strand. Ago2 protein selects the guide strand and cleaves its RNA target at the phosphodiester bond positioned between nucleotides 10 and 11 [32,35]. The resulting products are rapidly degraded because of the unprotected ends, and the passenger strand is also degraded [36,37]. The targeted RNA dissociates from the siRNA after the cleavage, and the RISC cleaves additional targets, resulting in decrease of expression of the target gene (Figure 1) [38].

Polo-like kinase-1

To develop RNAi therapy against cancers, it is essential that suitable gene targets are selected. Such targets include antiapoptotic proteins, cell cycle regulators, transcription factors, signal transduction proteins, and factors associated with malignant biological behaviors of cancer cells. All of these genes are associated with the poor prognosis of cancer patients. PLKs belong to the family of serine/threonine kinases and are highly conserved among eukaryotes. PLK family has identified PLK-1, PLK-2 (SNK), PLK-3 (FNK), and PLK-4 (SAK) in mammalians so far and PLKs function as regulators of both cell cycle progression and cellular response to DNA damage [19,39-41]. PLK-1 has an N-terminal serine/threonine protein kinase domain and two polo box domains at the C-terminal region. Polo box domains regulate the kinase activity of PLK-1 [21,42]. PLK-1 regulates cell division at several points in the mitotic phase: mitotic entry through CDK1 activation, bipolar spindle formation, chromosome alignment, segregation of chromosomes, and cytokinesis [19,43]. *PLK-1* gene expression is regulated during cell cycle progression, with a peak level occurring at M phase. Similar to its gene expression, PLK-1 protein expression and its activity are low in G0, G1, and S phases, and begin to increase in G2 phase with peak in M phase [44-47].

Whereas PLK-1 is scarcely detectable in most adult tissues [45,48,49], PLK-1 is overexpressed in cancerous tissues. Its expression levels were tightly correlated with

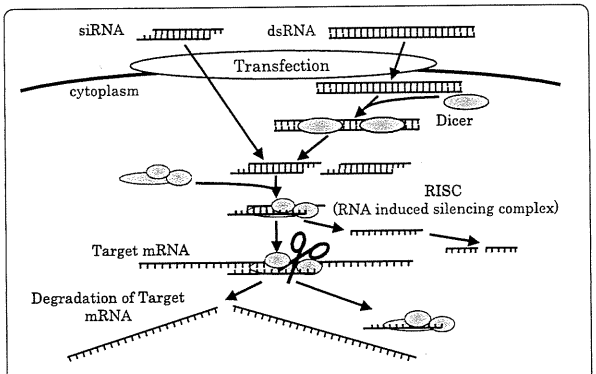

Figure 1 Mechanisms of RNA interference. After the introduction of dsRNA into a target cell, the dsRNA is processed into siRNA length of 21-23 nucletides by Dicer. siRNA then enters an RNA-induced silencing complex (RISC) assembly pathway. The dsRNA unwinds to form two single-strands of RNA. The passenger strand rapidly degrades and the guide strand binds and cleaves the target mRNA, resulting in mRNA degradation.

histological grades of tumors, clinical stages, and prognosis of the patients. PLK-1 mRNA levels were elevated in NSCLC tissues and this transcript levels were correlated with the survivals of cancer patients [50]. Moreover, the immunohistoligical study showed that PLK-1 protein was overexpressed in NSCLC tissues in patients at progressed stages of cancer (postsurgical stage ≥II) and in patients with poorly differentiated NSCLCs [51]. Patients with urinary bladder cancers expressing high levels of PLK-1 have a poor prognosis compared with patients with its low expression. Moreover, the histologically high-grade, deeply invasive, lymphatic-invasive, and venous-invasive bladder cancers demonstrated significantly higher PLK-1 expression [52]. As PLK-1 is overexpressed in other various cancers [21], PLK-1 overexpression is a prognostic biomarker for cancer patients.

Inhibition of PLK-1 activity induces mitotic arrest and tumor cell apoptosis [53-55]. Depletion of *PLK-1* mRNA also inhibits the functions of PLK-1 protein in DNA damages and spindle formation and causes the inhibition of the cell proliferation in a time- and a dose-dependent manner. PLK-1 siRNA treatment induces an arrest at the G2/M phase in the cell cycle with the increase of CDC2/Cyclin B1 [51,52,56,57]. PLK-1 siRNA-transfected cells had dumbbell-like and misaligned nuclei, indicating that PLK-1 depletion induced abnormalities of cell division during M phase, and these cells were shown to yield to caspase-dependent apoptosis [51,52,56]. As mentioned above, the kinases of PLK family cooperatively act in mitosis. Quantitative real-time RT-PCR data showed that PLK-2 and PLK-3 transcripts were increased after PLK-1 siRNA treatment [51]. Unlike PLK-1, PLK-2 and PLK-3 play inhibitory roles. PLK-2 is regulated by p53 and PLK-3 is activated by the DNA damage checkpoint [40]. These observations suggest that PLK-1 depletion induced mitotic catastrophe and activation of spindle checkpoint and DNA damage checkpoint, resulting in increased transcription of PLK-2 and PLK-3. Consequently, these PLK family kinases cooperatively prevented G2/M transition and induction of apoptosis. Importantly, depletion of PLK-1 does not affect the proliferation of normal cells although PLK-1 plays an important role in cell division [51,53,58]. This suggests that some other kinases compensate loss of PLK-1 function during mitosis in normal cells [51,58]. Collectively, PLK-1 could be an excellent target for cancer therapy.

Atelocollagen

Although siRNA target molecules are overexpressed in cancer cells, most of them are essential to maintain homeostasis of physiological functions in humans. Therefore, siRNAs must be delivered selectively into cancer cells. Moreover, naked siRNAs are degraded by endogenous nucleases when administered *in vivo*, so that delivery methods that protect siRNAs from such degradation are essential. For these reasons, safer and more effective DDSs must be developed. DDSs are divided into two categories: viral vector based carriers, and non-viral based carriers. Viral vectors are highly efficient delivery systems and they are the most powerful tools for transfection so far. However, viral vectors have several critical problems in *in vivo* application. Especially, retroviral and lentiviral vectors have major concerns of insertional mutagenesis [59,60]. Consequently, non-viral DDSs have been strenuously developed [11-13].

Atelocollagen, one of powerful non-viral DDSs, is type I collagen obtained from calf dermis [61]. The molecular weight of atelocollagen is approximately 300,000 and the length is 300 nm. It forms a helix of 3 polypeptide chains. Amino acid sequences at the N- and C-termini of the collagen molecules are called telopeptide, and they have antigenecity of collagen molecules. As the telopeptide is removed from collagen molecules by pepsin treatment, atelocollagen shows low immunogenicity. Therefore, atelocollagen has been shown to be a suitable biomaterial with an excellent safety profile and it is used clinically for a wide range of purposes. Atelocollagen is positively charged, which enable binding to negatively charged nucleic acid molecules, and bind to cell membranes. Moreover, at low temperature atelocollagen exists in liquid form, which facilitates easy mixing with nucleic acid solutions. The size of the atelocollagen-nucleic acid complex can be varied by altering the ratio of siRNA to atelocollagen. Because atelocollagen naturally forms a fiber-like structure under physiological conditions, particles formed a high concentration of atelocollagen persist for an extended period of time at the site of introduction, which is advantageous to achieve a sustained release of the associated nucleic acid. Atelocollagen is eliminated through a process of degradation and absorption similar to the metabolism of endogenous collagen [61]. Alternatively, particles formed under conditions of low atelocollagen concentrations result in siRNA/atelocollagen complexes approximately 100-300 nm in size that are suitable for systemic delivery by intravenous administration. Atelocollagen complexes protect siRNA from degradation by nucleases and are transduced efficiently into cells, resulting in long-term gene silencing. For instance, Takeshita et al. demonstrated that the systemic siRNA delivery with atelocollagen existed intact for at least 3 days in tumor tissues using a mouse model [62].

Preclinical application of RNAi therapy against PLK-1 in a murine advanced lung cancer model

Here we introduce an application of PLK-1 siRNA against an advanced lung cancer. As described above,

PLK-1 is overexpressed in NSCLC tumors. Liver metastasis is one of the most important prognostic factors in lung cancer patients [8,9,63,64]. However, despite the development of new chemotherapeutic and molecular targeting agents, current therapies are not sufficient to inhibit liver metastasis. We investigated the effects of PLK-1 siRNA on the liver metastasis of lung cancers using atelocollagen as a DDS. We first established a mouse model of liver metastasis. Spleens were exposed to allow direct intrasplenic injections of Luciferase (Luc)-labeled A549 NSCLC cells. Ten minutes after injections of tumor cells, the spleens were removed. After Luc-labeled A549 cell engraftment was confirmed by using *In Vivo* Imaging System (IVIS) of bioluminescence imaging [65], PLK-1 siRNA/atelocollagen complex, nonsense siRNA/atelocollagen complex, or PBS/atelocollagen complex was administered by intravenous injection for 10 consecutive days following day 1 of transplantation. On day 35, mice treated with nonsense siRNA/atelocollagen complex or PBS/atelocollagen complex showed extensive metastases in the liver when compared to mice treated with PLK-1 siRNA/atelocollagen complex (Figure 2). Moreover, on day 70 after the inoculation of tumor cells, livers of mice treated with nonsense siRNA/atelocollagen or PBS/atelocollagen complex had numerous large tumor nodules, whereas the livers of mice treated with PLK-1 siRNA/atelocollagen complex showed a much lower number of smaller nodules. These findings indicate that PLK-1 siRNA/atelocollagen complex is an attractive therapeutic tool for further development as a treatment against liver metastasis of lung cancer [51]. Consequently, our preclinical applications suggest that PLK-1 siRNA is a promising tool for cancer therapy.

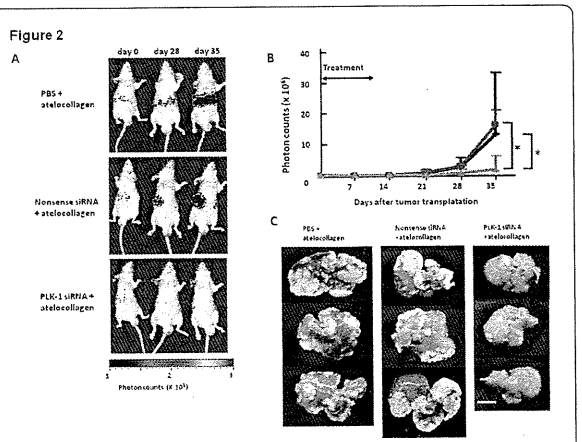

Figure 2 Application of PLK-1 RNAi therapy against liver metastatic NSCLC (cited from [51]). A. PBS/atelocollagen complex, nonsense siRNA/atelocollagen complex, or PLK-1 siRNA/atelocollagen complex was administered by intravenous injection. Representative mice showing bioluminescence after siRNA treatment. The photon counts of each mouse are indicated by the pseudocolor scales. B. Growth curves of inoculated Luc-labeled A549 cells measured by the IVIS (pink square, nonsense siRNA/atelocollagen complex (25 μg siRNA)-treated mice; blue diamond, PBS/atelocollagen complex-treated mice; orange triangle, PLK-1 siRNA/atelocollagen complex (25 μg siRNA)-treated mice; n = 5 for each group. On day 35 after inoculation, the luminesecence in the PLK-1 siRNA/atelocollagen-treated mice was significantly suppressed compared with that in other groups. * $p < 0.05$. Mean ± SD. C. Macroscopic analysis of mice livers after day 70 of inoculation. White nodules are metastatic liver tumors. Treatment with PLK-1 siRNA (25 μg) remarkably inhibited the growth of liver metastases compared with PBS or nonsense siRNA treatments (25 μg).

Conclusion

Our preclinical studies demonstrated that RNAi therapy against PLK-1 using atelocollagen is effective against liver metastatic NSCLC cancers. Recently, several clinical trials for cancer therapy are ongoing (Additional file 1: Table S1, http://clinicaltrials.gov/ct2/home). Although RNAi shows excellent specificity in gene-silencing, several adverse effects including activation of immune reaction [66,67] and off-target effects (induction of unintended gene silencing) [68] are brought in *in vivo* application. Safer and more efficient DDSs for systemic delivery are warranted to be developed. Moreover, studies to establish the pharmacokinetics and pharmacodynamics of siRNAs on the administration are necessary steps in the potential approval of siRNA as a tool for cancer therapy. To maximize efficacy and to minimize adverse effects of RNAi, it should be determined whether siRNAs are best administered alone or in combination with chemotherapeutic agents [69,70], and whether it is better to administer a single specific siRNA or multiple specific siRNAs [57,71-73]. In conclusion, RNAi therapy represents a powerful strategy against advanced lung cancers and may offer a novel and attractive therapeutic option. The success of RNAi depends on the suitable selection of target genes and the development of DDSs. We anticipate that the continued development of effective DDSs and the accumulation of evidence further proving the success of siRNA treatment will advance RNAi as a promising strategy for lung cancer therapy.

Additional material

Additional file 1: Table S1 Clinical trials of RNAi.

Lists of abbreviations

Ago: Argonaute; DDSs: drug delivery systems; dsRNA: double-strand RNA; EGFR: epidermal growth factor receptor; IVIS: *In Vivo* Imaging System; Luc: Luciferase; NSCLC: non-small cell lung cancer; nt: nucleotide; PAZ: Piwi/Argonaute/Zwille; PLK-1: Polo-like kinase-1; RISC: RNA-induced silencing complex; RNAi: RNA interference; siRNA: small interfering RNA; TKI: Tyrosine kinase inhibitor

Acknowledgements
This work was supported by a Grant-in-Aids for Scientific Research from the Ministry of the Education, Culture, Sports, Science, and Technology of Japan.

Author details
[1]Department of Transfusion Medicine and Cell Therapy, Kyoto University Hospital, Kyoto, Japan. [2]Division of Internal Medicine, Kyoto Second Red Cross Hospital, Kyoto, Japan. [3]Department of Molecular Cell Physiology, Kyoto Prefectural University of Medicine, Kyoto, Japan.

Authors' contributions
EK carried out our all experiments concerning this review and drafted the manuscript. EA designed our all experiments, carried out *in vivo* experiments, and wrote this review. TM supervised our research and wrote this review. All authors read and approved the final draft.

Competing interests
The authors declare that they have no competing interests.

Received: 16 October 2010 Accepted: 20 January 2011
Published: 20 January 2011

References

1. Parkin DM, Bray F, Ferlay J, Pisani P: **Global cancer statistics, 2002.** *CA Cancer J Clin* 2005, **55**:74-108.
2. Visbal AL, Leighl NB, Feld R, Shepherd FA: **Adjuvant Chemotherapy for Early-Stage Non-small Cell Lung Cancer.** *Chest* 2005, **128**:2933-2943.
3. Rudd R: **Chemotherapy in the treatment of non-small-lung cancer.** *Respiratory Disease in Practice* 1991, **7**:12-14.
4. Sharma SV, Bell DW, Settleman J, Haber DA: **Epidermal growth factor receptor mutations in lung cancer.** *Nat Rev Cancer* 2007, **7**:169-181.
5. Oxnard GR, Miller VA: **Use of erlotinib or gefitinib as initial therapy in advanced NSCLC.** *Oncology (Williston Park)* 2010, **24**:392-399.
6. Kobayashi S, Boggon TJ, Dayaram T, Janne PA, Kocher O, Meyerson M, Johnson BE, Eck MJ, Tenen DG, Halmos B: **EGFR mutation and resistance of non-small-cell lung cancer to gefitinib.** *N Engl J Med* 2005, **352**:786-792.
7. Pao W, Miller VA, Politi KA, Riely GJ, Somwar R, Zakowski MF, Kris MG, Varmus H: **Acquired resistance of lung adenocarcinomas to gefitinib or erlotinib is associated with a second mutation in the EGFR kinase domain.** *PLoS Med* 2005, **2**:e73.
8. Bremnes RM, Sundstrom S, Aasebo U, Kaasa S, Hatlevoll R, Aamdal S: **The value of prognostic factors in small cell lung cancer: results from a randomised multicenter study with minimum 5 year follow-up.** *Lung Cancer* 2003, **39**:303-313.
9. Hoang T, Xu R, Schiller JH, Bonomi P, Johnson DH: **Clinical model to predict survival in chemonaive patients with advanced non-small-cell lung cancer treated with third-generation chemotherapy regimens based on eastern cooperative oncology group data.** *J Clin Oncol* 2005, **23**:175-183.
10. Fire A, Xu S, Montgomery MK, Kostas SA, Driver SE, Mello CC: **Potent and specific genetic interference by double-stranded RNA in Caenorhabditis elegans.** *Nature* 1998, **391**:806-811.
11. Bumcrot D, Manoharan M, Koteliansky V, Sah DW: **RNAi therapeutics: a potential new class of pharmaceutical drugs.** *Nat Chem Biol* 2006, **2**:711-719.
12. Weichert W, Denkert C, Schmidt M, Gekeler V, Wolf G, Kobel M, Dietel M, Hauptmann S: **Polo-like kinase isoform expression is a prognostic factor in ovarian carcinoma.** *Br J Cancer* 2004, **90**:815-821.
13. Oh YK, Park TG: **siRNA delivery systems for cancer treatment.** *Adv Drug Deliv Rev* 2009, **61**:850-862.
14. Ochiya T, Takahama Y, Nagahara S, Sumita Y, Hisada A, Itoh H, Nagai Y, Terada M: **New delivery system for plasmid DNA in vivo using atelocollagen as a carrier material: the Minipellet.** *Nat Med* 1999, **5**:707-710.
15. Song E, Zhu P, Lee SK, Chowdhury D, Kussman S, Dykxhoorn DM, Feng Y, Palliser D, Weiner DB, Shankar P, *et al*: **Antibody mediated in vivo delivery of small interfering RNAs via cell-surface receptors.** *Nat Biotechnol* 2005, **23**:709-717.
16. Zimmermann TS, Lee AC, Akinc A, Bramlage B, Bumcrot D, Fedoruk MN, Harborth J, Heyes JA, Jeffs LB, John M, *et al*: **RNAi-mediated gene silencing in non-human primates.** *Nature* 2006, **441**:111-114.
17. Whitehead KA, Langer R, Anderson DG: **Knocking down barriers: advances in siRNA delivery.** *Nat Rev Drug Discov* 2009, **8**:129-138.
18. Judge AD, Bola G, Lee AC, MacLachlan I: **Design of noninflammatory synthetic siRNA mediating potent gene silencing in vivo.** *Mol Ther* 2006, **13**:494-505.
19. Barr FA, Sillje HH, Nigg EA: **Polo-like kinases and the orchestration of cell division.** *Nat Rev Mol Cell Biol* 2004, **5**:429-440.
20. Strebhardt K: **Multifaceted polo-like kinases: drug targets and antitargets for cancer therapy.** *Nat Rev Drug Discov* 2010, **9**:643-660.
21. Strebhardt K, Ullrich A: **Targeting polo-like kinase 1 for cancer therapy.** *Nat Rev Cancer* 2006, **6**:321-330.
22. Takai N, Hamanaka R, Yoshimatsu J, Miyakawa I: **Polo-like kinases (Plks) and cancer.** *Oncogene* 2005, **24**:287-291.
23. Ghildiyal M, Zamore PD: **Small silencing RNAs: an expanding universe.** *Nat Rev Genet* 2009, **10**:94-108.
24. Martin SE, Caplen NJ: **Applications of RNA interference in mammalian systems.** *Annu Rev Genomics Hum Genet* 2007, **8**:81-108.
25. Tomari Y, Zamore PD: **Perspective: machines for RNAi.** *Genes Dev* 2005, **19**:517-529.
26. Bernstein E, Caudy AA, Hammond SM, Hannon GJ: **Role for a bidentate ribonuclease in the initiation step of RNA interference.** *Nature* 2001, **409**:363-366.
27. Collins RE, Cheng X: **Structural domains in RNAi.** *FEBS Lett* 2005, **579**:5841-5849.
28. Hutvagner G, McLachlan J, Pasquinelli AE, Balint E, Tuschl T, Zamore PD: **A cellular function for the RNA-interference enzyme Dicer in the maturation of the let-7 small temporal RNA.** *Science* 2001, **293**:834-838.
29. Grishok A, Pasquinelli AE, Conte D, Li N, Parrish S, Ha I, Baillie DL, Fire A, Ruvkun G, Mello CC: **Genes and mechanisms related to RNA interference regulate expression of the small temporal RNAs that control C. elegans developmental timing.** *Cell* 2001, **106**:23-34.
30. Ketting RF, Fischer SE, Bernstein E, Sijen T, Hannon GJ, Plasterk RH: **Dicer functions in RNA interference and in synthesis of small RNA involved in developmental timing in C. elegans.** *Genes Dev* 2001, **15**:2654-2659.
31. Lee YS, Nakahara K, Pham JW, Kim K, He Z, Sontheimer EJ, Carthew RW: **Distinct roles for Drosophila Dicer-1 and Dicer-2 in the siRNA/miRNA silencing pathways.** *Cell* 2004, **117**:69-81.
32. Elbashir SM, Lendeckel W, Tuschl T: **RNA interference is mediated by 21- and 22-nucleotide RNAs.** *Genes Dev* 2001, **15**:188-200.
33. Hammond SM, Bernstein E, Beach D, Hannon GJ: **An RNA-directed nuclease mediates post-transcriptional gene silencing in Drosophila cells.** *Nature* 2000, **404**:293-296.
34. Parker JS, Barford D: **Argonaute: A scaffold for the function of short regulatory RNAs.** *Trends Biochem Sci* 2006, **31**:622-630.
35. Elbashir SM, Martinez J, Patkaniowska A, Lendeckel W, Tuschl T: **Functional anatomy of siRNAs for mediating efficient RNAi in Drosophila melanogaster embryo lysate.** *Embo J* 2001, **20**:6877-6888.
36. Matranga C, Tomari Y, Shin C, Bartel DP, Zamore PD: **Passenger-strand cleavage facilitates assembly of siRNA into Ago2-containing RNAi enzyme complexes.** *Cell* 2005, **123**:607-620.
37. Liu J, Carmell MA, Rivas FV, Marsden CG, Thomson JM, Song JJ, Hammond SM, Joshua-Tor L, Hannon GJ: **Argonaute2 is the catalytic engine of mammalian RNAi.** *Science* 2004, **305**:1437-1441.
38. Ashihara E, Kawata E, Maekawa T: **Future prospect of RNA interference for cancer therapies.** *Curr Drug Targets* 2010, **11**:345-360.
39. Clay FJ, McEwen SJ, Bertoncello I, Wilks AF, Dunn AR: **Identification and cloning of a protein kinase-encoding mouse gene, Plk, related to the polo gene of Drosophila.** *Proc Natl Acad Sci USA* 1993, **90**:4882-4886.
40. Eckerdt F, Yuan J, Strebhardt K: **Polo-like kinases and oncogenesis.** *Oncogene* 2005, **24**:267-276.
41. Winkles JA, Alberts GF: **Differential regulation of polo-like kinase 1, 2, 3, and 4 gene expression in mammalian cells and tissues.** *Oncogene* 2005, **24**:260-266.
42. Jang YJ, Ma S, Terada Y, Erikson RL: **Phosphorylation of threonine 210 and the role of serine 137 in the regulation of mammalian polo-like kinase.** *J Biol Chem* 2002, **277**:44115-44120.
43. van de Weerdt BC, Medema RH: **Polo-like kinases: a team in control of the division.** *Cell Cycle* 2006, **5**:853-864.
44. Alvarez B, Martinez AC, Burgering BM, Carrera AC: **Forkhead transcription factors contribute to execution of the mitotic programme in mammals.** *Nature* 2001, **413**:744-747.

45. Lake RJ, Jelinek WR: **Cell cycle- and terminal differentiation-associated regulation of the mouse mRNA encoding a conserved mitotic protein kinase.** *Mol Cell Biol* 1993, **13**:7793-7801.
46. Lee KS, Yuan YL, Kuriyama R, Erikson RL: **Plk is an M-phase-specific protein kinase and interacts with a kinesin-like protein, CHO1/MKLP-1.** *Mol Cell Biol* 1995, **15**:7143-7151.
47. Uchiumi T, Longo DL, Ferris DK: **Cell cycle regulation of the human polo-like kinase (PLK) promoter.** *J Biol Chem* 1997, **272**:9166-9174.
48. Golsteyn RM, Schultz SJ, Bartek J, Ziemiecki A, Ried T, Nigg EA: **Cell cycle analysis and chromosomal localization of human Plk1, a putative homologue of the mitotic kinases Drosophila polo and Saccharomyces cerevisiae Cdc5.** *J Cell Sci* 1994, **107(Pt 6)**:1509-1517.
49. Hamanaka R, Maloid S, Smith MR, O'Connell CD, Longo DL, Ferris DK: **Cloning and characterization of human and murine homologues of the Drosophila polo serine-threonine kinase.** *Cell Growth Differ* 1994, **5**:249-257.
50. Wolf G, Elez R, Doermer A, Holtrich U, Ackermann H, Stutte HJ, Altmannsberger HM, Rubsamen-Waigmann H, Strebhardt K: **Prognostic significance of polo-like kinase (PLK) expression in non-small cell lung cancer.** *Oncogene* 1997, **14**:543-549.
51. Kawata E, Ashihara E, Kimura S, Takenaka K, Sato K, Tanaka R, Yokota A, Kamitsuji Y, Takeuchi M, Kuroda J, *et al*: **Administration of PLK-1 small interfering RNA with atelocollagen prevents the growth of liver metastases of lung cancer.** *Mol Cancer Ther* 2008, **7**:2904-2912.
52. Nogawa M, Yuasa T, Kimura S, Tanaka M, Kuroda J, Sato K, Yokota A, Segawa H, Toda Y, Kageyama S, *et al*: **Intravesical administration of small interfering RNA targeting PLK-1 successfully prevents the growth of bladder cancer.** *J Clin Invest* 2005, **115**:978-985.
53. Spankuch-Schmitt B, Bereiter-Hahn J, Kaufmann M, Strebhardt K: **Effect of RNA silencing of polo-like kinase-1 (PLK1) on apoptosis and spindle formation in human cancer cells.** *J Natl Cancer Inst* 2002, **94**:1863-1877.
54. Gumireddy K, Reddy MV, Cosenza SC, Boominathan R, Baker SJ, Papathi N, Jiang J, Holland J, Reddy EP: **ON01910, a non-ATP-competitive small molecule inhibitor of Plk1, is a potent anticancer agent.** *Cancer Cell* 2005, **7**:275-286.
55. Steegmaier M, Hoffmann M, Baum A, Lenart P, Petronczki M, Krssak M, Gurtler U, Garin-Chesa P, Lieb S, Quant J, *et al*: **BI 2536, a potent and selective inhibitor of polo-like kinase 1, inhibits tumor growth in vivo.** *Curr Biol* 2007, **17**:316-322.
56. Liu X, Erikson RL: **Polo-like kinase (Plk)1 depletion induces apoptosis in cancer cells.** *Proc Natl Acad Sci USA* 2003, **100**:5789-5794.
57. Judge AD, Robbins M, Tavakoli I, Levi J, Hu L, Fronda A, Ambegia E, McClintock K, MacLachlan I: **Confirming the RNAi-mediated mechanism of action of siRNA-based cancer therapeutics in mice.** *J Clin Invest* 2009, **119**:661-673.
58. Liu X, Lei M, Erikson RL: **Normal cells, but not cancer cells, survive severe Plk1 depletion.** *Mol Cell Biol* 2006, **26**:2093-2108.
59. Check E: **A tragic setback.** *Nature* 2002, **420**:116-118.
60. Hacein-Bey-Abina S, von Kalle C, Schmidt M, Le Deist F, Wulffraat N, McIntyre E, Radford I, Villeval JL, Fraser CC, Cavazzana-Calvo M, Fischer A: **A serious adverse event after successful gene therapy for X-linked severe combined immunodeficiency.** *N Engl J Med* 2003, **348**:255-256.
61. Sano A, Maeda M, Nagahara S, Ochiya T, Honma K, Itoh H, Miyata T, Fujioka K: **Atelocollagen for protein and gene delivery.** *Adv Drug Deliv Rev* 2003, **55**:1651-1677.
62. Takeshita F, Minakuchi Y, Nagahara S, Honma K, Sasaki H, Hirai K, Teratani T, Namatame N, Yamamoto Y, Hanai K, *et al*: **Efficient delivery of small interfering RNA to bone-metastatic tumors by using atelocollagen in vivo.** *Proc Natl Acad Sci USA* 2005, **102**:12177-12182.
63. Schiller JH, Harrington D, Belani CP, Langer C, Sandler A, Krook J, Zhu J, Johnson DH: **Comparison of four chemotherapy regimens for advanced non-small-cell lung cancer.** *N Engl J Med* 2002, **346**:92-98.
64. Sandler A, Gray R, Perry MC, Brahmer J, Schiller JH, Dowlati A, Lilenbaum R, Johnson DH: **Paclitaxel-carboplatin alone or with bevacizumab for non-small-cell lung cancer.** *N Engl J Med* 2006, **355**:2542-2550.
65. Nogawa M, Yuasa T, Kimura S, Kuroda J, Sato K, Segawa H, Yokota A, Maekawa T: **Monitoring luciferase-labeled cancer cell growth and metastasis in different in vivo models.** *Cancer Lett* 2005, **217**:243-253.
66. Behlke MA: **Progress towards in vivo use of siRNAs.** *Mol Ther* 2006, **13**:644-670.
67. Marques JT, Williams BR: **Activation of the mammalian immune system by siRNAs.** *Nat Biotechnol* 2005, **23**:1399-1405.
68. Jackson AL, Burchard J, Schelter J, Chau BN, Cleary M, Lim L, Linsley PS: **Widespread siRNA "off-target" transcript silencing mediated by seed region sequence complementarity.** *Rna* 2006, **12**:1179-1187.
69. von Bueren AO, Shalaby T, Oehler-Janne C, Arnold L, Stearns D, Eberhart CG, Arcaro A, Pruschy M, Grotzer MA: **RNA interference-mediated c-MYC inhibition prevents cell growth and decreases sensitivity to radio- and chemotherapy in childhood medulloblastoma cells.** *BMC Cancer* 2009, **9**:10.
70. Shi Z, Liang YJ, Chen ZS, Wang XH, Ding Y, Chen LM, Fu LW: **Overexpression of Survivin and XIAP in MDR cancer cells unrelated to P-glycoprotein.** *Oncol Rep* 2007, **17**:969-976.
71. Shi XH, Liang ZY, Ren XY, Liu TH: **Combined silencing of K-ras and Akt2 oncogenes achieves synergistic effects in inhibiting pancreatic cancer cell growth in vitro and in vivo.** *Cancer Gene Ther* 2009, **16**:227-236.
72. Honma K, Iwao-Koizumi K, Takeshita F, Yamamoto Y, Yoshida T, Nishio K, Nagahara S, Kato K, Ochiya T: **RPN2 gene confers docetaxel resistance in breast cancer.** *Nat Med* 2008, **14**:939-948.
73. Mu P, Nagahara S, Makita N, Tarumi Y, Kadomatsu K, Takei Y: **Systemic delivery of siRNA specific to tumor mediated by atelocollagen: Combined therapy using siRNA targeting Bcl-xL and cisplatin against prostate cancer.** *Int J Cancer* 2009, **125**:2978-2990.

doi:10.1186/2043-9113-1-6
Cite this article as: Kawata *et al.*: RNA interference against polo-like kinase-1 in advanced non-small cell lung cancers. *Journal of Clinical Bioinformatics* 2011 1:6.

ELSEVIER

The Journal of
Heart and Lung
Transplantation

http://www.jhltonline.org

CLINICAL DILEMMAS

ABO-incompatible living-donor lobar lung transplantation

Tsuyoshi Shoji, MD,[a] Toru Bando, MD,[a] Takuji Fujinaga, MD,[a] Fengshi Chen, MD,[a] Kimiko Yurugi,[b] Taira Maekawa, MD,[b] and Hiroshi Date, MD[a]

From the Departments of [a]Thoracic Surgery and [b]Transfusion Medicine and Cell Therapy, Kyoto University, Kyoto 606-8507, Japan.

KEYWORDS:
lung transplantation;
ABO-incompatible;
living-donor;
bronchiolitis obliterans;
bone marrow transplantation

ABO-incompatible living-donor lobar lung transplantation was performed in a 10-year-old boy with bronchiolitis obliterans (BO) after bone marrow transplantation (BMT) for recurrent acute myeloid leukemia (AML). His blood type had changed from AB to O since he underwent BMT and he had no anti-A/B antibody, and received type B and AB donor lobar lungs. To our knowledge, this case represents the first successful living-donor lobar lung transplantation from ABO-incompatible donors.
J Heart Lung Transplant 2011;30:479–80

ABO-incompatible organ transplantation, especially kidney and liver transplantation, have been performed in an effort to overcome the donor organ shortage. However, very few cases have been reported involving ABO-incompatible lung transplantation, and there has been only one intentional lung transplant reported so far. Herein we report ABO-incompatible lung transplantation in a 10-year-old boy with bronchiolitis obliterans (BO) after bone marrow transplantation (BMT).

Case report

A 6-year-old boy was diagnosed with acute myeloid leukemia (AML) in 2005 and was treated with chemotherapy. In May 2008, at 9 years of age, he underwent BMT from an unrelated, HLA-identical, ABO-mismatched donor for recurrent AML. His blood type was originally AB(+) and, after receiving BMT from a blood type O(+) donor, his blood type changed to O(+). In early 2009, at 9 of age, he began complaining of dyspnea and was diagnosed with BO, with the presumption that the cause was pulmonary graft-vs-host disease (GVHD). Respiratory distress continued to worsen with respiratory *Pseudomonous aeruginosa* infection despite home oxygen therapy.

In January 2010, at 10 years of age, the patient was transferred to Kyoto University Hospital. On admission, his vital capacity was 0.72 liter (39.6% predicted), forced expiratory volume in 1 second (FEV_1) was 0.27 liter (16.3% predicted), and arterial blood gas showed pH 7.40, PaO_2 = 87.0 mm Hg and $PaCO_2$ = 55.8 mm Hg, with 2 liters/min oxygen administered via a nasal cannula.

Cadaveric lung transplantation was not a realistic option because brain death is accepted only for persons >15 years of age in Japan. His parents, a mother, 43 years old, ABO type AB(+), and father, 44 years old, ABO type B(+), each offered to be lung donors. The patient's ABO type had changed to type O according to ABO testing of red cells, but ABO serum test did not detect any anti-A/B antibody in his serum and tolerance to A and B antigens had been established. After careful discussion, we concluded that the risk of an ABO-incompatible lung transplant in this particular case would be equivalent to that of an ABO-compatible transplant, because the production of anti-A and anti-B antibody would be unlikely even if new A and B antigen was presented from the donor after lung transplantation.

In February 2010, the patient underwent living-donor lobar lung transplantation with a left lower lobe from his mother and a right lower lobe from his father. The surgical aspects of the donor lobectomy, donor back-table preservation technique and recipient bilateral pneumonectomy and lobar implantation have been described previously by Starnes and colleagues.[1] For peri-operative transfusion, type O red blood cells and type AB fresh-frozen plasma and platelets were used for the recip-

Reprint requests: Tsuyoshi Shoji, MD, Department of Thoracic Surgery, Kyoto University, 54 Shogoin-Kawahara-cho, 54 Shogoin Kawahara-cho, Sakyo-ku, Kyoto 606-8507, Japan. Telephone: +81-75-751-4975. Fax: +81-75-751-4974.
E-mail address: tshoji@kuhp.kyoto-u.ac.jp

1053-2498/$ -see front matter
doi:10.1016/j.healun.2010.10.015

ients. Post-operative immunosuppression included cyclosporine, mycophenolate mofetil and prednisone.

Post-operative course was relatively uneventful. The patient was completely weaned from the ventilator on post-operative day (POD) 3. There was transient, very weak detection of anti-A antibody (Table 1). However, there was no apparent acute cellular rejection (ACR) or antibody-mediated rejection (AMR) post-operatively. Because there was no clinical finding suggesting rejection, no lung biopsy was performed post-operatively.

He was discharged from the hospital on POD 75. At that time, arterial blood gas in room air showed pH 7.43, PaO_2 = 92.6 mm Hg and $PaCO_2$ = 37.6 mm Hg. FVC was 1.53 liters (83.2% predicted) and FEV_1 was 1.12 liters (67.9% predicted) (Table 2). Five months post-operatively, he returned to a normal life without oxygen inhalation and is able to perform daily activities.

Discussion

After bone marrow transplantation, if the patient has received marrow from a compatible but dissimilar ABO type, serum antibodies will not agree with red cell antigens. Our pediatric patient, who was originally type AB, received type O marrow, had circulating type O red cells, but produced no anti-A/B antibody in the serum at the time of lung transplantation. According to ABO testing of red cells, recipient (type O) donors (B and AB) ABO-type matching was incompatible; however, because the recipient had no anti-A/B antibody in serum, we could perform this surgical procedure with ABO-incompatible donors. Other possible hematologic changes that could occur in the recipient after lung transplantation were carefully discussed. Theoretically, the lymphocytes derived from the type B lung donor could produce anti-A antibodies in the recipient, and not only attack the recipient's other organs, which were originally type AB, but also attack contralateral type AB donor lung. However, there was only transient weak detection of anti-A antibodies and no AMR occurred post-operatively.

Recently, many cases of ABO-incompatible organ transplantation, especially kidney and liver transplantation, have been performed to overcome the donor organ shortage. Japanese groups reported excellent patient and graft survival in ABO-incompatible kidney transplantation using regimens consisting of plasmapheresis, immunosuppression, immunoabsorption and splenectomy, showing similar outcomes to those of ABO-compatible donor transplants.[2,3] However, intentional ABO-incompatible lung transplantation was reported in only one case.[4] Pierson et al reported 42 instances (0.4%) of accidental ABO-incompatible lung transplantation among 9,804 primary lung transplants, according to the database of the Organ Procurement and Transplant Network in the USA,[5] and the outcomes were acceptable compared with those of ABO-compatible lung transplants when the intensive therapy was used as just described.

Although the present case showed a unique blood type background because of prior bone marrow transplantation, to our knowledge, this case represents the first successful living-donor lobar lung transplantation from ABO-incompatible donors. Although the short-term outcome was satisfactory, long-term follow-up is needed to determine whether this procedure is ultimately justified.

Table 1 Serologic Analysis of Anti-A and -B Antibody for Recipient

	Days post-transplant						
	Pre	7	12	19	26	54	82
Aggregation to type A RBC	0	W+[a]	0	W+	W+	0	0
Aggregation to type B RBC	0	0	0	0	0	0	0

RBC, red blood cells.
[a]Very weak aggregation.

Table 2 Time Trend of Pulmonary Function Test for Recipient

	Days post-transplant		
	Pre	82	188
Height (cm)	127.0	127.4	128.0
Body weight (kg)	24.0	25.0	28.0
VC (liters)	0.72	1.62	1.61
FVC (liters)	0.72	1.53	1.60
FEV_1 (liters)	0.27	1.12	1.09

Disclosure statement

The authors have no conflicts of interest to disclose.

References

1. Starnes VA, Barr ML, Cohen RG, et al. Living-donor lobar lung transplantation experience: intermediate results. J Thorac Cardiovasc Surg 1996;112:1284-90.
2. Aikawa A, Ohara T, Arai K, et al. Clinical outcome and accommodation in ABO incompatible kidney transplantation. Clin Transpl 2004:135-42.
3. Takahashi K, Saito K, Takahara S, et al. Excellent long-term outcome of ABO-incompatible living donor kidney transplantation in Japan. Am J Transplant 2004;4:1089-96.
4. Struber M, Warnecke G, Hafer C, et al. Intentional ABO-incompatible lung transplantation. Am J Transplant 2008;8:2476-8.
5. Pierson RN III, Moore J, Merion RM, et al. ABO-incompatible lung transplantation. Amsterdam: Elsevier; 2006:63-9.

ELSEVIER

Nanomedicine: Nanotechnology, Biology, and Medicine
7 (2011) 889–895

Research Article

nanomedicine
Nanotechnology, Biology, and Medicine

nanomedjournal.com

Single-step, label-free quantification of antibody in human serum for clinical applications based on localized surface plasmon resonance

Junta Yamamichi, MS, MPH[a,b], Tetsunori Ojima, MS[a], Kimiko Yurugi[c], Mie Iida, MS[a], Takeshi Imamura, MS[a], Eishi Ashihara, MD, PhD[c], Shinya Kimura, MD, PhD[c,d,*], Taira Maekawa, MD, PhD[c]

[a]*High Performance Sensing Research Division, Frontier Research Center, Canon Inc., Tokyo, Japan*
[b]*Department of Biostatistics, Boston University School of Public Health, Boston, Massachusetts*
[c]*Department of Transfusion Medicine and Cell Therapy, Kyoto University Hospital, Kyoto, Japan*
[d]*Division of Hematology, Respiratory Medicine and Oncology, Department of Internal Medicine, Faculty of Medicine, Saga University, Saga, Japan*

Received 24 August 2010; accepted 1 February 2011

Abstract

The amount of antibody in blood is an important measure of health status for making critical decisions in clinical practice. Here, we demonstrated a single-step, label-free, molecular diagnositic method based on localized surface plasmon resonance (LSPR) using standard 96-well microtiter plates. We improved the LSPR biosensor so that it can measure antibodies to blood group antigens in human serum with a single-step operation. First, we employed the ampholytic polymeric surface modification technique to present an efficient molecular scaffold on the sensor surface. Second, we selected the combination of an appropriate reference molecule against the antigen and a blocking agent to significantly reduce the variability of signal due to nonspecific responses of the unknown in the sample. Finally, we overcame the analytical difficulty arising from serum and achieved a single-step "wash-free" measurement of the amount of target antibody in human serum.

From the Clinical Editor: In this paper, a novel, single-step, label-free, molecular diagnositic method is discussed for antibody detection based on localized surface plasmon resonance using standard 96-well microtiter plates.

Key words: Optical biosensor; Localized surface plasmon resonance; Immunoassay; Blood test

In clinical tests, antibody titers in blood are very important measures for diagnosis. Antibodies related to infectious diseases such as chickenpox or hepatitis are among the conventional targets of those tests. In autoimmune diseases such as rheumatoid arthritis or systemic lupus erythematosus, autoantibodies play an important role in diagnosis as well. Other examples like blood group ABO-related immunoglobulin levels after living-donor organ transplantations are critically essential for treatments and prognosis of transplantees because antibody-mediated rejection is one of the primary causes of poor outcomes.[1] Several methods are used to measure antibody levels in serum. They include enzyme-linked immunosorbent assay (ELISA), radioimmunoassay (RIA), and fluorescence-activated flow cytometry (FACS). Moreover, among the various new types of chemical and biological sensors, the optical method using surface plasmon resonance (SPR) on planar gold films has made a particularly important contribution to affinity-based biosensing applications, including antigen-antibody reactions, during the past two decades. As mentioned in the reviews,[2-4] the SPR sensor has been widely used to monitor the change in the refractive index induced by a broad range of analyte bindings in a label-free manner. This direct detection method of biomolecules eliminates conventional signal transducers such as fluorophore and enzyme.

In our previous work,[5,6] we showed that the SPR method could be used to measure anti-human blood group A (anti-A) IgG titers in sera rapidly and quantitatively while avoiding the interference from IgM-type antibodies. This could be a promising tool because one of the clinical interests is the amount of IgG-type antibodies. Measurement of anti-A IgG titers in sera has been routinely conducted by the conventional test tube (TT) method. This method, however, has the intrinsic problem of interexaminer variability because it relies on visual observation.[7] Our study was the initial trial for clinical use of the SPR method.

The authors declare no conflict of interest.

*Corresponding author.
E-mail address: shkimu@cc.saga-u.ac.jp (S. Kimura).

1549-9634/$ – see front matter © 2011 Elsevier Inc. All rights reserved.
doi:10.1016/j.nano.2011.02.002

Please cite this article as: J., Yamamichi, et al, Single-step, label-free quantification of antibody in human serum for clinical applications based on localized surface plasmon resonance. *Nanomedicine: NBM* 2011;7:889-895, doi:10.1016/j.nano.2011.02.002

It improved the diagnostic operation by intermittently monitoring the level of the same patients' antibodies after clinical ABO-unmatched transplant.

However, because the SPR method is based on flow-cell type sensor chips, the resultant sequential operation is very complex and a more efficient procedure is desired in clinical practice. This instrumental characteristic possibly limits the reduction of the total assay time and the achievement of a high-throughput assay system. In addition, the SPR method detects unknown species, not only in the vicinity of the sensing planar gold surface, but at a relatively long distance from its surface. This can cause unpredictable and unnecessary responses of signals that affect the accuracy of the measurement and mandate the temperature control of the whole system to minimize the fluctuation of the refractive index. Therefore, signal compensations such as a reference flow cell or subsequent washing are necessary. Moreover, it requires us to regenerate a sensor chip surface before another test is to be done. It is quite a complex process to prepare the new sensor chip surface with the same sensor characteristics as previous ones. From the analytical viewpoint, these properties are not favorable to control the quality of each measurement in the long run.

In this article, inspired by the similarity to the SPR method and its less practical applicability, we further explore the possibility of the application of the localized surface plasmon resonance (LSPR) method[8] to this kind of measurement. As one of the promising technologies to acquire the information of molecular binding events, this method can be made with very simple set-up and assay procedures in comparison with those of SPR. Through the advance of nanofabrication techniques and nanophotonics, this particular label-free immunoassay has been widely investigated for many biological applications.[9-14] Previously, we have demonstrated its simple fabrication in a 96-well microtiter plate format and its applicability to a label-free immunoassay with the expectation that this method can be used in clinical tests.[15] We have found the density of immobilized gold nanoparticles (AuNPs) best to detect antibody in sample solution.

When metal nanoparticles are excited by light, their conduction electrons on the surface, known as surface plasmons, exhibit collective oscillations. These oscillations result in both absorption and scattering of incident light of a specific resonant wavelength. This phenomenon is called LSPR. The characteristic resonance energy of the surface plasmon is strongly dependent on the dielectric properties of the local environment around the nanometric particles.[16,17] Thus, small changes in the refractive index induced by surrounding liquid or analyte binding at or near the surface of nanometric particles can be measured as shifts in the LSPR spectra. We believe that the LSPR method has the benefits of both SPR and ELISA. These include a label-free simple assay like SPR and a high-throughput parallel operation like ELISA.

To our knowledge, our investigation is the first clinical application of the LSPR method with human blood samples. We measured anti-A IgG levels in human serum based on LSPR to compare with the previously established methods by SPR. Our study focused on simplicity, reproducibility and accuracy with respect to the clinical diagnosis. One of the difficulties in the label-free methodology is reducing the nonspecific responses from serum to increase the intensity of specific response. For this purpose, we employed novel zwitterionic copolymer to serve as a molecular scaffold on the surface of AuNPs. It can adsorb strongly onto the gold surface with static ionic interaction between its amino groups and gold and present efficient grafting points for further chemical modification on the surface of NPs, such as immobilization of antigen groups or blocking agents through its carboxyl groups, which would eventually lead to the improvement of signal intensity. Due to the improved signal intensity, the final measurements can be done even without removing and washing the serum before the measurements. We call this the "wash-free" measurement that simplifies the process as a single-step assay of a specific analyte in serum. Putting the test solution into a reaction well could be the only required operation to achieve accurate diagnostic results. Finally, for validation of our method, comparison of the results with several other diagnostic methods was also performed.

Methods

Functionalization of the surface of AuNPs

Ninety six-well polystyrene amine surface microtiter plates (Corning, Corning, New York) were used as the substrates on which the AuNPs (100 nmϕ; BBInternational, Cardiff, United Kingdom) were immobilized at the optimized density.[15] The surface of AuNPs were functionalized with polyampholite polymer PAS-410 (Nitto Boseki, Fukushima, Japan) and human blood group A trisaccharide antigen molecules (Carbohydrate Synthesis, Oxford, United Kingdom). Details in preventing nonspecific adsorption are described in the Supplementary Material, available online at http://www.nanomedjournal.com.

LSPR measurement of the levels of target antibody (anti-A)

Serum samples were taken from 41 healthy adult volunteers at Kyoto University Hospital, including 21 men and 20 women with informed consents according to the Declaration of Helsinki. Crude human serum was diluted by one third, using a diluent containing 0.26% PAS-410 and 0.01% BSA in phosphate buffered saline (PBS) (pH 7.0) to prepare the test solution. Without dilution, some samples were within the range of saturation of signal. Therefore, we decided to dilute all crude samples in this work. The diluent consisted of components similar to those on the surface of AuNPs, and we aimed to avoid unnecessary interaction between the sample and sensor surface. A 100 μL aliquot of the test solution was then incubated for 30 minutes at room temperature (24–25°C). Next, we measured its optical extinction spectrum in the "wash-free" condition. Subsequently, each well was washed and filled with 100 μL PBS. The optical extinction spectrum was measured again in the "wash" condition. The specific peak shift induced by the antibodies bound to immobilized antigens was obtained by subtracting the peak shift of the reference-well measured at the same point in time. With the purified anti-A IgG diluted in PBS, we created a plot of concentration-dependent shift of spectrum peak (λ_{max}) to estimate concentrations of the antibodies in the test solution. In addition, a

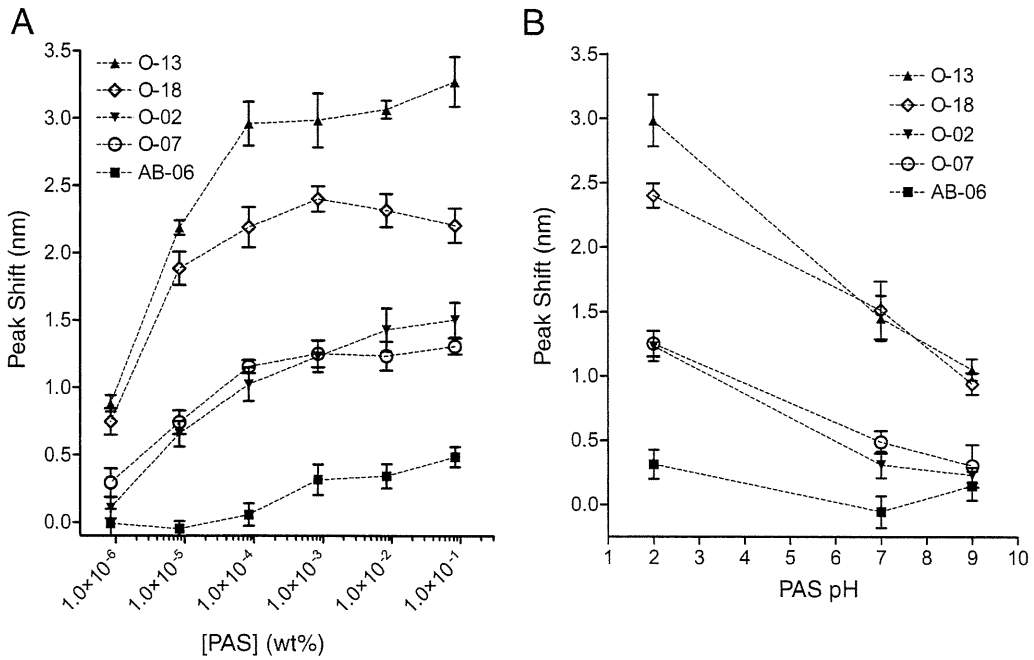

Figure 1. Effect of coating polymer concentrations and pH levels on sensor responses (spectrum peak (λ_{max}) shift). **(A)** Effect of concentration. **(B)** Effect of pH level. Data was acquired using the sera from 4 blood group O and 1 blood group AB volunteers. Error bars represent standard errors.

secondary analysis was performed to quantify bound IgG-type antibodies by adding a 100 μL aliquot of 100 μg/mL goat anti-human IgG monoclonal antibody (Rockland Immunochemicals, Gilbertsville, Pennsylvania) and incubating for 30 minutes at 37°C. The final spectra measurement was performed after being completely dried with compressed dried air. A plate reader (Varioskan; Thermo Fisher Scientific, Waltham, Massachusetts) was used to measure the optical extinction spectra of immobilized AuNPs on the plates. The spectra data were analyzed by fitting them to a Gaussian curve to identify a spectrum peak (IGOR Pro; WaveMetrics, Portland, Oregon).

Determination of antibody levels by the TT and SPR method and their correlation with those measured by the LSPR method

We employed the same procedure described elsewhere for the TT and SPR measurements.[5,6] For the SPR method, we used Biacore X system (GE Healthcare, Amersham, United Kingdom). The blood group A trisaccharide antigen molecules were immobilized on the sensor chip CM5 following the standard procedures. An anti-human IgG monoclonal antibody (Sanbio, Uden, The Netherlands) diluted with the running buffer HBS-EP (GE Healthcare) was used to measure the amounts of anti-A IgG associated with the blood group antigen A immobilized on the chip. All measurements were performed at 25°C. The deviations among different sensor chips were adjusted using the responses from the identical serum sample. We performed a statistical evaluation of correlation of the results from 3 methods. We computed linear correlations of both the TT and SPR methods with the LSPR method (SAS 9.1 software; SAS Institute, Cary, North Carolina).

Results

Sensor functionalization and assay optimization

Our sensor elements consisted of monodisperse AuNPs, which were immobilized on the surface of polystyrene microtiter plates as reported in our previous work.[15] Microtiter plates are very useful for multiplexing the assay on the same plate. Fundamentally, our LSPR method is characterized by determining shifts of λ_{max}, which are the measure of changes in the refractive index at or near the proximity of the surface of AuNPs. These shifts are induced by specific analyte binding to target elements on the surface of AuNPs and are to be converted into the actual amount of analyte molecules bound on the surface using the standard response curve. Spectrum measurement was done by standard plate reader. The surface of AuNPs was first coated with the polyampholytic polymer anchored on their surface by its amino groups. The polymer is a novel water-soluble zwitterionic copolymer composed of diallylamine hydrochloride salt and maleic acid. This polymer provides us with efficient grafting points for the target element of human blood group A trisaccharide antigen through its carboxyl groups. The characteristics of the polyampholytic polymer are strongly affected by pH levels, which in turn change the sensor properties. Thus, at first we evaluated the sensing properties in terms of signal intensity with various pH levels and concentrations of the polymer solution to achieve good selectivity (Figure 1). We used 5 representative human sera for this optimization, including 4 blood group O and 1 blood group AB. Although the variation of the concentration of anti-A in serum is relatively large even in healthy volunteers, it may due to the difference in individual exposure to the antigen. The serum of blood group AB works as a negative control

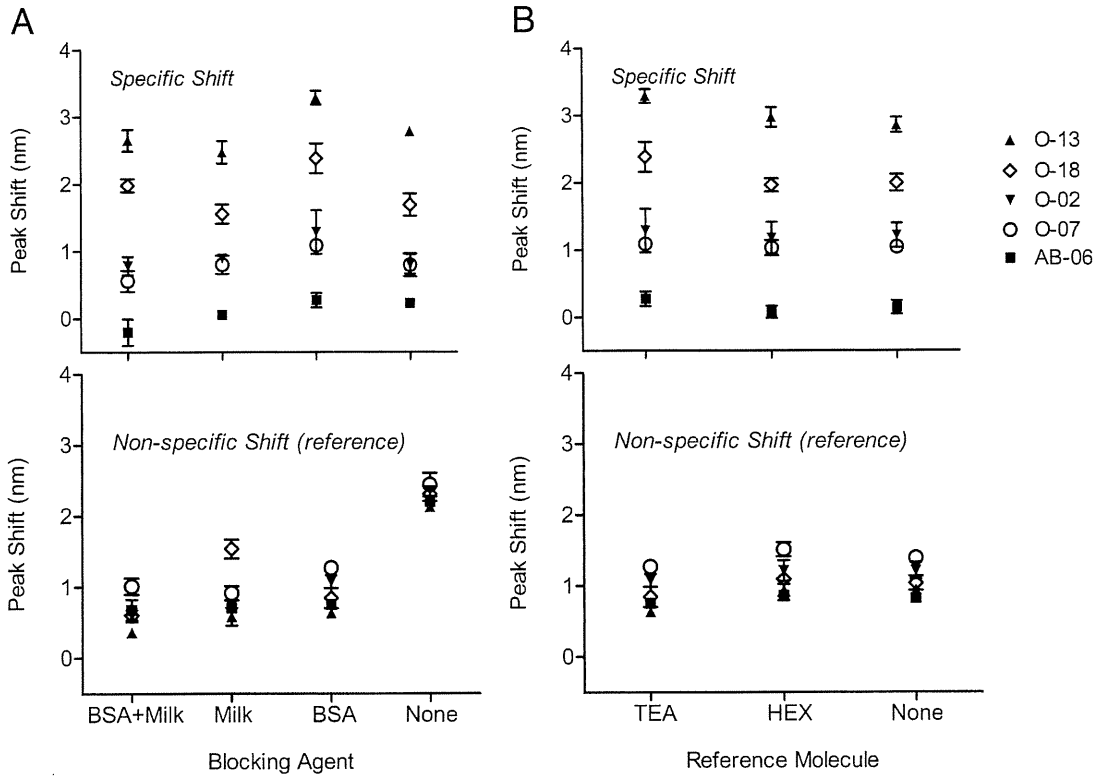

Figure 2. Comparison of effects of blocking agents and reference molecules on sensor responses (shift of λ_{max}). **(A)** Effect of blocking agents: BSA+Skim milk, Skim milk, BSA and None. **(B)** Effect of reference molecules: TEA, HEX and None. The upper graphs represent data from signal wells, whereas the lower graphs represent data from reference wells. Data were acquired using the sera from 4 blood group O and 1 blood group AB volunteers. Error bars represent standard errors.

because we do not expect any response to the blood group A antigen from the serum of blood group AB. We chose the optimum condition for coating as 8.4×10^{-4} % (w/w) at pH 2.0 hereafter, which was in the middle of the stable condition having a large response.

In the second step of the optimization, we further investigated the selection of blocking agents and reference molecules, which would reduce the unknown signals from crude samples and enable a single-step, label-free measurement. We tried well-known blocking agents of BSA, skim milk and their combination. For reference molecules, which were immobilized on the surface of AuNPs in the reference well, we tried TEA and HEX. Based on the result shown in Figure 2, we conclude that choosing BSA and TEA for blocking agent and reference molecule, respectively, can achieve larger signal. Then, we were convinced that the optimum condition of our assay had been achieved and we were ready to proceed to measure various serum samples. Again, we observed a good selectivity towards anti-A antibody also in this optimized condition by using serum of blood group AB.

Validation: Concentration-dependent shifts of λ_{max} by purified human anti-A antibody

We confirmed concentration-dependent shifts of λ_{max} as basic characteristics of our LSPR sensor using purified target antibody: human anti-A antibody (Figure 3). We fitted this profile assuming a 1:1 binding model between anti-A and blood group A antigen. The fitted curve provides us the dissociation constant (K_d) of 1.5×10^{-4} g/mL. Due to the difficulty of preparing a higher concentration of purified anti-A antibody from human blood, we did not measure λ_{max} in a higher concentration range than 40 μg/mL. However, with using the serum that has the highest concentration of anti-A antibody, we observed the similar trend of shifts of λ_{max} across our experimental concentration range.

Challenge: single-step, wash-free measurement of serum samples

We applied our assay to the various samples from volunteers and investigated the applicability of a single-step measurement in crude samples. The difference between the process of "wash" and "wash-free" measurement concerns whether we replace the serum in each well with a buffer solution before performing the spectrum measurement. In the single-step "wash-free" measurement, we do not discard the serum and we proceed directly to the spectrum measurement. The major purpose of this "wash" operation is to significantly reduce the signal from the unknown species in the serum and improve the accuracy of the measurement. Figure 4 compares the signals from both operations. Interestingly, the slope of linear regression between 2 methods is identical to unity with $R^2 = 0.91$. This means that there is no significant difference between them. We therefore conclude that the single-step "wash-free" measurement works

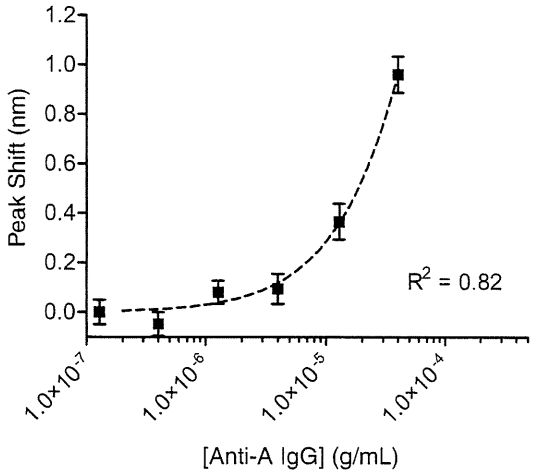

Figure 3. Anti-A concentration-dependent shifts of λ_{max}. Dotted line shows a sigmoidal fitting to the experimental data. Error bars represent standard errors from 8 samples.

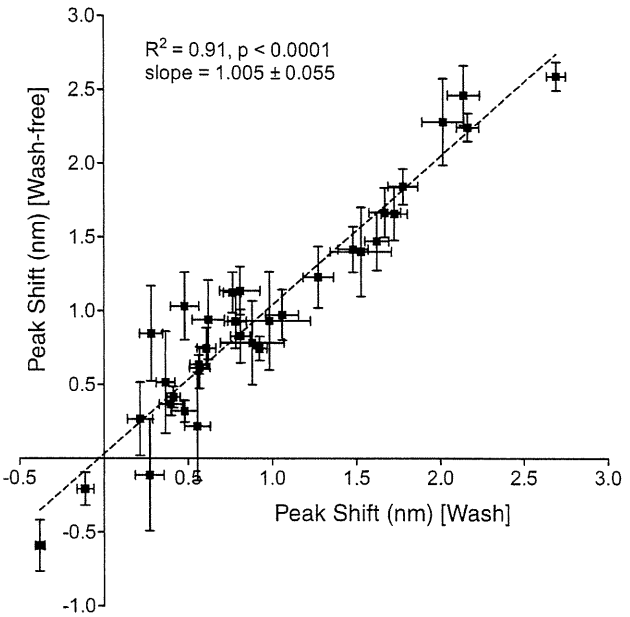

Figure 4. Wash-free measurement. Correlation between "wash-free" and "wash" measurements. Dotted line was determined by linear regression analysis (slope = 1.005, R^2 = 0.91). Error bars represent standard errors.

equivalently to the standard "wash" operation without any significant interference from the serum in the well.

Comparison of the single-step assay with other methods

Finally, we compared our single-step "wash-free" assay with other methods, i.e., TT and SPR, using the common 41 serum samples (Figure 5, *A*). Because two major isotypes of antibodies exist in serum, i.e., IgG and IgM-types, we conducted a supplemental measurement using the secondary antibody (anti-human IgG) that specifically detects the amount of IgG-type anti-A antibody bound on the AuNPs and computed the correlations separately in those two types of measurements (Table 1). As for the TT method, the procedure we used for the computation of correlations is generally assumed to measure IgG-type antibody only. We observed at least moderately strong correlations among the methods. For the IgG-type antibody, the correlation coefficient between LSPR and TT is smaller than that observed between LSPR and SPR (0.66 vs. 0.79). This is possibly due to the less quantitative nature of the TT method, in which results are discrete values. For instance, the TT results of many samples were zero in Figure 5, *B*. On the other hand, correlation coefficients between LSPR and SPR are approximately 0.8 (strong) for both types of measurement, and more than 60% of the variability in the LSPR results is explained statistically by SPR (Figure 5, *A*). In particular, we did not find a difference in the correlations between the measurements of total antibody and IgG-type in the comparison of LSPR and SPR. Thus, we conclude that LSPR and SPR measured the similar types of antibody in our assay because two types of measurements (i.e., total and IgG-type antibody) did not change the correlation between the two methods.

Discussion

Development of a rapid, accurate and sensitive diagnostic method is favored in clinical practices from both financial and ethical points of view. With this goal, many types of new biosensors have been proposed and presented to the clinical community for use in diagnostics. Meanwhile, TT and ELISA have been widely used along with accumulated empirical evidence and increased confidence, even though they require sophisticated operations and substantial time to complete. We believe that one of the tipping points where the clinical community will accept a new method depends on the extent of its simplicity of operation and reproducibility of results relative to the conventional methods.

In this study, we demonstrated a more efficient approach to quantify the amount of antibodies in sera while fulfilling practical requirements. We optimized our assay to detect antibodies in both nano-optical[15] and surface chemical aspects as shown in Figures 1 and 2. The optimal arrangement of immobilized AuNPs and the use of a polyampholytic polymer are two essential elements of our method. The former enhanced the sensitivity and the latter enabled efficient surface chemistry and high selectivity. Though the zwitterionic copolymer looks difficult to control in a stable manner, we found its optimum condition to facilitate surface modification. We believe that larger signal responses using the acidic polymer solution are caused by the dense attachment of the polymer on the surface of AuNPs due to static attraction between positively charged polymer chains and negatively charged AuNPs. The capability of blocking nonspecific binding is similar for BSA and skim milk (Figure 2), but we cannot expect a synergetic effect using both materials simultaneously. From our experience, BSA seems to be a more stable agent for long-term storage. To optimize a reference well, we tried 2 kinds of molecules (i.e., TEA and HEX). As expected, slightly better trends were achieved using more hydrophilic molecules, which have a relatively similar

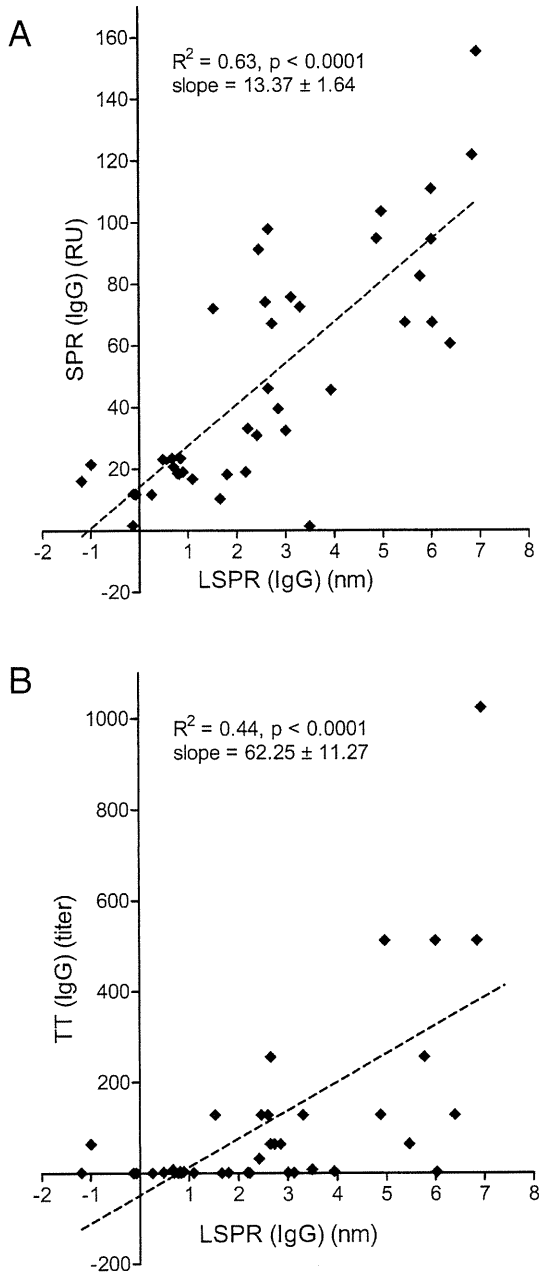

Figure 5. Correlations between TT, SPR and LSPR measurements of 41 volunteers. **(A)** Between SPR (IgG) and LSPR (IgG). Dotted line was determined by linear regression analysis (slope = 13.37, R^2 = 0.63). **(B)** Between TT (IgG) and LSPR (IgG). Dotted line was determined by linear regression analysis (slope = 62.25, R^2 = 0.44).

molecular characteristic to the trisaccharide antigen. Attained sensitivity and selectivity both contributed to the success of single-step "wash-free" measurement. A calibration plot of λ_{max} as a function of anti-A antibody concentration shows a detection limit of <10 μg/mL (Figure 3). This plot is based on the specific shift subtracted by nonspecific shift. Thus, a lower bound of error bar should simply exceed zero at the detection limit. Using a streptavidin-biotin reaction in diluted human blood, Wang et al

Table 1
Pearson correlation coefficients between assays

	TT (IgG)	SPR (Total)	SPR (IgG)
LSPR (Total)	0.70	0.80	0.78
LSPR (IgG)	0.66	0.80	0.79

The correlation coefficients were computed with the data from the common 41serum samples.

obtained a detection limit of about 3 μg/mL.[13] We are convinced that our results are within a reasonable range using an antigen-antibody reaction.

In comparison with other methods, we observed at least moderately strong correlations among them (Table 1). A statistical interpretation of R-squares is that at most, 44% and 63% of variability of the results in LSPR were to be explained by TT and SPR, respectively (Figure 5). In other words, we should be cautious about considering other factors that influence the measurements. This is because such methods do not necessarily measure exactly the same events that LSPR measures. Particularly, TT is less quantitative, for which results are discrete values based on serial dilutions and visual observation. Moreover, SPR uses a flow-cell system, which means it detects a dynamic process of binding events, not a static process. These diferences would contribute to the decreased correlations or R–squares.

It is well known that human serum has several isotypes of antibody dominated by IgG and IgM, which was confirmed by the TT method here. We consider it in the case of our assay. We suppose that LSPR and SPR detect mostly the IgG-type antibody, which we presume from their similar responses even without the use of the secondary antibody. That secondary antibody was used to distinguish IgG and IgM. This is, to some extent, due to the higher K_d of IgM antibodies in a monovalent intereraction[18] between antigen-binding region and immobilized antigen than that of IgG. In our assay by LSPR or SPR, IgG and IgM competed against each other for the same targeting antigen. Our observation of results, however, is that the major responses are caused by the reaction of IgG, owing to its higher affinity to the antigen than IgM. Therefore, we conclude that LSPR could substitute for the function of SPR in measuring antibody titers and improve the operability in clinical practice because of their similar diagnostic characteristics in terms of the isotypes of antibody to be measured.

Two features of our method are worth mentioning with respect to the clinical diagnostics. First, our assay is simple, and a single-step operation is possible. Figure 4 reveals the equivalency of responses between "wash" and "wash-free" measurements. The near-zero intercept also indicates the competence of our technique to prevent nonspecific adsorption from serum contents. This is owing to the spatial characteristic of the LSPR biosensor as illustrated in the Graphical Abstract. Specifically, LSPR has a smaller sensing volume than SPR, which is appropriate to exclusively detect the surface binding events. In addition, we have optimized the sensing volume for detecting antibodies as reported previously.[15] We emphasize this property because none of the conventional methods is able to measure quantitatively with a single step. This observation would bring a huge benefit in clinical practice because the only required

procedure to get accurate diagnostic results is to put the test solution into a reaction well. This means a substantial reduction of total operational time to measure the concentration of antibodies. In addition, it could eliminate other laborious manual steps like washing wells, which can cause deviation in the responses obtained by many laboratory technicians in clinical practice. Furthermore, intermittent monitoring of specific markers in the sample could be easily conducted in a clinical setting using our method because the quality of each measurement well can be precisely controlled. For example, monitoring the change in the amount of anti-human blood group antigen antibodies is essential for prognosis after the ABO-unmatched transplant. The risk of adverse events in the case of ABO-incompatible living-liver transplantation would decrease significantly with timely monitoring and appropriate remedies. With the help of our methods, physicians will have better opportunities to more accurately follow up on patients' critical responses to the transplants than in the past.

Second, as our assay used microtiter plates, we are easily able to multiplex the measurement because the required sample is small and the operation is simple. In many situations, physicians are interested in a set of different antibodies or biomolecules to improve the performance of diagnosis of a patient's condition. For instance, multiplexed markers for autoimmune diseases or tumors are used and explored.[19-22]

Further intensive study is necessary to improve this assay. A major drawback to our demonstrated method is the use of reference wells, which is also a fundamental challenge in the development of label-free optical biosensors. This duplicates the operation to improve signal intensity. However, we hope to find a way to obtain accurate results even without reference wells. Moreover, this single-well measurement will provide a real-time measurement of molecular binding events, which enables us to understand the affinity and kinetics of that binding event similarly by the SPR method.

In conclusion, we have shown a single-step, label-free quantification of anti-A antibodies in human serum. Our method achieved a simple, efficient and reliable way to specifically detect antibodies in crude serum samples. These results point to the vast applicability of our LSPR method to measure the level of antibodies in the test solution by adopting various kinds of antigens immobilized on AuNPs. We believe that the LSPR method will have the potential to be routinely used as a rapid and cost-effective diagnostic method in the future.

Appendix A. Supplementary data

Supplementary data to this article can be found online at doi:10.1016/j.nano.2011.02.002.

References

1. Egawa H, Teramukai S, Haga H, Tanabe M, Fukushima M, Shimazu M. Present status of ABO-Incompatible living donor liver transplantation in Japan. Hepatology 2008;47:143-52.
2. Homola J, Yee SS, Gauglitz G. Surface plasmon resonance sensors: review. Sens Actuators B: Chem 2000;63:24-30.
3. Englebienne P, Van Hoonacker A, Verhas M. Surface plasmon resonance: principles, methods and applications in biomedical sciences. Spectrosc 2003;17:255-73.
4. Campbell CT, Kim G. SPR microscopy and its applications to high-throughput analyses of biomolecular binding events and their kinetics. Biomater 2007;28:2380-92.
5. Kimura S, Yurugi K, Segawa H, Kuroda J, Sato K, Nogawa M, et al. Rapid quantitation of immunoglobulin G antibodies specific for blood group antigens A and B by surface plasmon resonance. Transfusion 2005;45:56-62.
6. Yurugi K, Kimura S, Ashihara E, Tsuji H, Kawata A, Kamitsuji Y, et al. Rapid and accurate measurement of anti-A/B IgG antibody in ABO-unmatched living donor liver transplantation by surface plasmon resonance. Transfusion Med 2007;17:97-106.
7. Kobayashi T. Standardization of the assay method for anti-A/B antibody titers and its problems. Int Congress Series 2006;1292:3-7.
8. Anker JN, Hall WP, Lyandres O, Shah NC, Zhao J, Van Duyne RP, et al. Biosensing with plasmonic nanosensors. Nat Mater 2008; 7:442-53.
9. Nath N, Chilkoti AA. Colorimetric Gold nanoparticle sensor to interrogate biomolecular interactions in real time on a surface. Anal Chem 2002;74:504-9.
10. Englebienne P. Use of colloidal gold surface plasmon resonance peak shift to infer affinity constants from the interactions between protein antigens and antibodies specific for single or multiple epitopes. Analyst 1998;123:1599-603.
11. Haes AJ, Chang L, Klein WL, Van Duyne RP. Detection of a biomarker for Alzheimer's disease from synthetic and clinical samples using a nanoscale optical biosensor. J Am Chem Soc 2005;127:2264-71.
12. Mayer KM, Lee S, Liao H, Rostro BC, Fuentes A, Scully PT, et al. A label-free immunoassay based upon localized surface plasmon resonance of gold nanorods. ACS Nano 2008;2:687-92.
13. Wang Y, Qian W, Tan Y, Ding S. A label-free biosensor based on gold nanoshell monolayers for monitoring biomolecular interactions in diluted whole blood. Biosens Bioelectron 2008;23:1166-70.
14. Endo T, Kerman K, Nagatani N, Takamura Y, Tamiya E. Label-free detection of peptide nucleic acid-DNA hybridization using localized surface plasmon resonance based optical biosensor. Anal Chem 2005;77:6976-84.
15. Yamamichi J, Iida M, Ojima T, Handa Y, Yamada T, Kuroda R, et al. The mesoscopic effect on label-free biosensors based on localized surface plasmon resonance of immobilized colloidal gold. Sens Actuators B: Chem 2009;143:349-56.
16. Kelly KL, Coronado E, Zhao LL, Schatz GC. The optical properties of metal nanoparticles: the influence of size, shape, and dielectric environment. J Phys Chem B 2003;107:668-77.
17. Miller MM, Lazarides AA. Sensitivity of metal nanoparticle plasmon resonance band position to the dielectric environment as observed in scattering. J Opt A: Pure Appl Opt 2006;8:S239-49.
18. Strandh M, Ohlin M, Borrebaeck CAK, Ohlson S. New approach to steroid separation based on a low affinity IgM antibody. J Immunol Methods 1998;214:73-9.
19. Döner T, Hansen A. Autoantibodies in normals - the value of predicting rheumatoid arthritis. Arthritis Res Ther 2004;6:282-4.
20. Hanly JG, Thompson K, McCurdy G, Fougere L, Theriault C, Wilton K. Measurement of autoantibodies using multiplex methodology in patients with systemic lupus erythematosus. J Immunol Methods 2010;352: 147-52.
21. Binder S. Autoantibody Detection Using Multiplex Technologies. Lupus 2006;15:412-21.
22. Vojdani A. Antibodies as predictors of complex autoimmune diseases and cancer. Int J Immunopathol Pharmacol 2008;21:553-66.

Oncogene (2011) 30, 2789–2797

www.nature.com/onc

ORIGINAL ARTICLE

Combined effects of novel heat shock protein 90 inhibitor NVP-AUY922 and nilotinib in a random mutagenesis screen

T Tauchi[1], S Okabe[1], E Ashihara[2], S Kimura[3], T Maekawa[4] and K Ohyashiki[1]

[1]First Department of Internal Medicine, Tokyo Medical University, Tokyo, Japan; [2]Department of Molecular Cell Physiology, Kyoto Prefectural University of Medicine, Kyoto, Japan; [3]Division of Hematology, Respiratory Medicine and Oncology, Department of Internal Medicine, Faculty of Medicine, Saga University, Saga, Japan and [4]Department of Transfusion Medicine and Cell Therapy, Faculty of Medicine, Kyoto University, Kyoto, Japan

To overcome imatinib resistance, more potent ABL tyrosine kinase inhibitors (TKIs), such as nilotinib and dasatinib have been developed, with demonstrable preclinical activity against most imatinib-resistant BCR–ABL kinase domain mutations, with the exception of T315I. However, imatinib-resistant patients already harboring mutations have a higher likelihood of developing further mutations under the selective pressure of potent ABL TKIs. NVP-AUY922 (Novartis) is a novel 4,5-diaryloxazole adenosine triphosphate-binding site heat shock protein 90 (HSP90) inhibitor, which has been shown to inhibit the chaperone function of HSP90 and deplete the levels of HSP90 client protein including BCR–ABL. In this study, we investigated the combined effects of AUY922 and nilotinib on random mutagenesis for BCR–ABL mutation (Blood, 109; 5011, 2007). Compared with single agents, combination with AUY922 and nilotinib was more effective at reducing the outgrowth of resistant cell clones. No outgrowth was observed in the presence of 2 μM of nilotinib and 20 nM of AUY922. The observed data from the isobologram indicated the synergistic effect of simultaneous exposure to AUY922 and nilotinib even in BaF3 cells expressing BCR–ABL mutants including T315I. *In vivo* studies also demonstrated that the combination of AUY922 and nilotinib prolonged the survival of mice transplanted with mixture of BaF3 cells expressing wild-type BCR–ABL and mutant forms. Taken together, this study shows that the combination of AUY922 and nilotinib exhibits a desirable therapeutic index that can reduce the *in vivo* growth of mutant forms of BCR–ABL-expressing cells.
Oncogene (2011) **30,** 2789–2797; doi:10.1038/onc.2011.3; published online 31 January 2011

Keywords: BCR–ABL; tyrosine kinase inhibitor; nilotinib; HSP90; T315I

Correspondence: Dr T Tauchi, First Department of Internal Medicine, Tokyo Medical University, 6-7-1 Nishishinjuku, Shinjuku-ku, Tokyo 160-0023, Japan.
E-mail: tauchi@tokyo-med.ac.jp
Received 10 February 2010; revised 15 November 2010; accepted 1 January 2011; published online 31 January 2011

Introduction

Resistance to the ABL tyrosine kinase inhibitor (TKI), imatinib, in Ph-positive leukemia is often caused by selection of mutations in BCR–ABL kinase domain altering residues that are directly or indirectly critical for imatinib binding (O'Hare *et al.*, 2007). To overcome imatinib resistance, more potent ABL TKIs, such as nilotinib and dasatinib have been developed, with demonstrable preclinical activity against most imatinib-resistant BCR–ABL kinase domain mutations, with the exception of T315I (Shah *et al.*, 2004; Weisberg *et al.*, 2005). The T315I is the single most frequent mutation that outgrows and leads to relapse during nilotinib and imatinib-treatment (Jabbour *et al.*, 2008). Other mutations, however, are found to have emerged at the time of relapse in ABL TKI-resistant patients (Branford *et al.*, 2009). F359V and the P-loop mutants Y253H and E255K/V are associated with relapse to nilotinib, and F317A/L and V299L are found in dasatinib-resistant patients (Branford *et al.*, 2009). Imatinib-resistant patients already harboring mutations have a higher likelihood of developing further mutations under the selective pressure of ABL TKIs (Garg *et al.*, 2009). The challenge for development of an effective Ph-positive leukemia therapy is therefore to develop an alternative treatment strategy that does not rely solely on kinase domain inhibition but rather results in degradation of the offending BCR–ABL protein regardless of its mutation status.

NVP-AUY922 is a novel 4,5-diaryloxazole adenosine triphosphate-binding site heat shock protein 90 (HSP90) inhibitor, which has been shown to inhibit the chaperone function of HSP90 and deplete the levels of HSP90 client protein (for example, ErbB2, Akt, Raf and Bcr–Abl) (Brough *et al.*, 2008; Eccles *et al.*, 2008; Stuhmer *et al.*, 2008). Combining AUY922 with ABL kinase inhibitors may provide several advantages, such as enhanced efficacy and reducing the potential emergence of new resistant mutations. In this study, we performed a comprehensive drug combination experiment using a broader range of concentrations for AUY922 and nilotinib or imatinib. Compared with single agents, combination with AUY922 and nilotinib was more effective at reducing the outgrowth of resistant cell clones. At the highest concentration of nilotinib, the